Mouse Hepatitis Virus Infection Induces a TLR2-Dependent Activation of Inflammatory Functions in Liver Sinusoidal Endothelial Cells during Acute Hepatitis

Christian Bleau, Aveline Filliol, Michel Samson, Lucie Lamontagne

MOUSE HEPATITIS VIRUS INFECTION INDUCES A TLR2-DEPENDENT ACTIVATION OF INFLAMMATORY FUNCTIONS IN LIVER SINUSOIDAL ENDOTHELIAL CELLS DURING ACUTE HEPATITIS

Christian Bleau[1], Aveline Filliol[2], Michel Samson[2], and Lucie Lamontagne[1]

[1]*Department of Biological Sciences, Université du Québec à Montréal, Montreal Canada, H3C 3P8;* [2]*U.1085 Inserm, IRSET, Institut de recherche en Santé-Environnement-Travail, Université de Rennes 1, 35043 Rennes, France*

Corresponding author

Dre Lucie Lamontagne DMV, Ph.D
Département Sciences Biologiques
Université du Québec à Montréal,
C.P. 8888 Succ. Centre-Ville
Montréal, Qué.
H3C 3P8

Tel : (514) 987-3000 poste 3184

Fax : (514) 987-4647
e-mail : lamontagne.lucie@uqam.ca

Running title: MHV3 reverts liver sinusoidal endothelial cell functions

Word count for the abstract: 254

Word count for the text: 8071

Key words: liver sinusoidal endothelial cell, mouse hepatitis virus, inflammation, tolerance, cytokines, chemokines, Fgl2, IL-33.

ABSTRACT

Under physiological conditions, the liver sinusoidal endothelial cells (LSECs) mediate hepatic immune tolerance towards self or foreign antigens through constitutive expression of anti-inflammatory mediators. However, upon viral infection or TLR2 activation, LSECs can achieve proinflammatory functions but their role in hepatic inflammation during acute viral hepatitis is unknown. Using the highly virulent mouse hepatitis virus (MHV) type 3 and the attenuated variants 51.6-MHV3 and YAC-MHV3, exhibiting lower tropism for LSECs, we investigated *in vivo* and *in vitro* the consequence of LSEC infection on their pro-inflammatory profile and the aggravation of acute hepatitis process. *In vivo* infection with virulent MHV3, in comparison to attenuated strains, resulted in fulminant hepatitis associated with higher hepatic viral load, tissue necrosis, levels of inflammatory mediators and earlier recuitement of inflammatory cells. Such hepatic inflammatory disorders correlated with disturbed production of IL-10 and vascular factors by LSECs. We next showed *in vitro* that infection of LSECs by the virulent MHV3 strain altered their production of anti-inflammatory cytokines and promoted higher release of pro-inflammatory and procoagulant factors and earlier cell damage in comparison to attenuated strains. This higher replication and pro-inflammatory activation in LSECs by the virulent MHV3 strain was associated with a specific activation of TLR2 signalling by the virus. We provided evidence that TLR2 activation of LSCEs by MHV3 is an aggravating factor of hepatic inflammation and correlates with the severity of hepatitis. Taken together, these results indicate that preservation of immunotolerant properties of LSECs during acute viral hepatitis is an imperative factor to limit hepatic inflammation and damages.

IMPORTANCE

Viral hepatitis B and C infections are serious health problem infecting over 350 million and 170 million people worldwide respectively. It has been suggested that a balance between protection and liver damage mediated by the host's immune response during the acute phase of infection would be determinant in hepatitis outcome. Thus, it appears crucial to identify the factors that predispose in exacerbating liver inflammation to limit hepatocyte injury. Liver sinusoidal endothelial cells (LSECs) can express both anti- and pro-inflammatory functions but their role in acute viral hepatitis has never been investigated. Using the mouse hepatitis virus (MHV) infections as animal models of viral hepatitis, we report for the first time that *in vitro* and *in vivo* infection of LSECs by the pathogenic MHV3 serotype leads to a reversion of their intrinsic anti-inflammatory phenotype towards a pro-inflammatory profile as well as disorders in vascular factors, correlating with the severity of hepatitis. These results highlight a new viral-promoted mechanism of exacerbation of liver inflammatory response during acute hepatitis.

INTRODUCTION

Under physiological conditions, the liver adopts mechanisms of immune tolerance towards innocuous gut-derived food and microbial antigens (such as LPS) to prevent undesired inflammatory responses. The induction of tolerance in the liver is mediated by several resident hepatic cells such as the endothelial cells lining the hepatic sinusoids (LSEC), the Kupffer cells (KC) and in a lesser extent the hepatocytes (1). However, LSECs tolerizing and anti-inflammatory functions were recently shown to be more efficient than those of KCs (2). Given their anatomical situation, LSECs are first in contact with portal-delivered antigens and thus act as a sieving barrier in expressing highly efficient sentinel and scavenger functions that contribute to clearance of microbial products (3). They also tightly control blood-parenchyma exchanges via a dynamic regulation of the sinusoidal blood flow in releasing vasoactive factors such as NO (reviewed in 4). LSECs play a major role in liver tolerance in displaying a restricted toll like receptor (TLR)-mediated activation profile to microbial products (5, 6) and producing high amounts of anti-inflammatory cytokines, such as tumor growth factor (TGF)-β and IL-10 (7, 8). However, upon viral infection or stimulation by TLR1/2 ligands, LSECs can switch towards an inflammatory and immunogenic state and induce recruitment of leucocytes and virus-specific CD8+ T cell immunity (5, 9). The role of LSECs in inflammatory liver diseases is poorly kown but as these cells can express both anti- and pro-inflammatory functions, they could act as moderator or rather exacerbator of liver inflammation.

Hepatitis B virus (HBV) and hepatitis C virus (HCV) infections are serious health problem affecting over 350 million and 170 million people worldwide respectively (10). Most liver damages in HBV/HCV infections are primarly attributed to an exuberant immunopathological response triggered by viral infection rather than direct injury caused by viral replication (11, 12). It has been suggested that the balance between protection and liver damage mediated by the host's immune response during the acute phase of infection would be critical in the outcome of hepatitis (13). Evidence suggests that an exacerbated hepatic inflammatory response during acute infection may predispose to the development of a fulminant hepatic failure characterized by extensive hepatocellular dysfunctions and high mortality (14). The role of LSECs in viral hepatitis is largely unknown and data are somewhat contradictory. Indeed, LSECs were suggested to contribute to the clearance of HCV and HBV from the bloodstream (15, 16) and to control HCV replication (17) or rather promote its transmission to hepatocytes in acting as a viral reservoir (18). Few data suggest that LSECs may also participate to hepatic inflammation since the fibrinogen-like factor 2 (Fgl-2), promoting vascular thrombosis and hepatic inflammation, and the proinflammatory alarmin IL-33, both produced by LSECs, are up-regulated in acute or chronic hepatitis (19-22). A better understanding of the role of LSECs during the acute phase of viral hepatitis may help to identify new mechanisms that predispose to inflammation-driven hepatocyte injury and liver failure.

The mouse hepatitis virus type 3 (MHV3), belonging to coronavirus family, is a relevant murine model to unravel the role of LSECs in acute viral hepatitis. MHV3 infects LSECs,

hepatocytes, Kupffer (KC) and Ito cells all expressing the carcinoembryonic antigen 1a (CEACAM1a) viral receptor and induces fulminant hepatitis leading to death of susceptible C57BL/6 mice within 3–4 days (23-25). LSECs are thought to play an important role in the resistance of A/J mice to MHV3 infection in controlling viral replication and delaying the transmission of the viral progeny to hepatocytes (26). Previous studies have reported early structural and vascular disorders in LSECs during MHV3 infection in susceptible C57Bl/6 mice. Indeed, a reduced number of fenestrations in liver sinusoids and a correlation between the fulminance of hepatitis and the induction of Fgl2 in LSECs have been described (27, 28). We have also shown that MHV3 infection was associated with early release of IL-33 by LSECs (29) and a reduction in the intrahepatic levels of immunosuppressive IL-10, PGE2 and TGF-β cytokines suggesting viral-induced disturbances in LSEC-mediated liver tolerance (30). Several attenuated MHV3 variants, such as the 51.6- and YAC-MHV3 viruses, have been *in vitro* generated to study the role of specific hepatic cells in hepatitis process. Compared to the parental MHV3, the major difference of the 51.6-MHV3 variant is its inefficiency to replicate in LSECs (24). Such difference is reflected by induction of milder hepatitis and higher hepatic levels of IL-10 and TGF-β (30). The YAC-MHV3 variant, showing lower tropism for LSECs and macrophages, induces a subclinical hepatitis characterized by few perivascular inflammatory foci (31) and higher induction of anti-inflammatory cytokines in the liver than 51.6-MHV3 (30). The absence of vascular thrombosis combined with efficient recruitment of mononuclear cells favor hepatic clearance of YAC-MHV3 and full recovery of infected mice within 15 days (32). These improved clinical outcomes in mice infected by the attenuated variants support the

hypothesis that preservation of structural and functional integrity of LSECs may be one determining factor in the severity of hepatitis.

In this study, we report that robust infection of LSECs by the highly virulent MHV3, in contrast to the attenuated 51.6- and YAC-MHV3 variants, promotes disturbances in their anti-inflammatory functions and secretion of vascular factors resulting in high release of inflammatory mediators and pro-coagulant Fgl-2 simultaneously with decrease in NO and IL-10 levels. Such MHV3-induced LSEC disorders correlated *in vivo* with higher hepatic inflammation, damages and viral replication as well as disturbances in leucocytes recruitment in mice infected by MHV3. We provide evidence that higher infection and proinflammatoy activation of LSECs by MHV3 was related to a specific viral induction of TLR2 signalling. The aggravating role for TLR2 in hepatic inflammation and LSEC disorders was confirmed in MHV3-infected TLR2 KO mice in which hepatic damages, pro- vs anti-inflammatory cytokines ratio and LSEC-derived IL-10 production were significantly improved.

MATERIALS AND METHODS

Mice:

Female C57BL/6 (Charles River, St-Constant, Qc, Canada) and TLR2 knock out (KO) (C57BL/6-129 $Tlr^{tm/Kir}$/J, Jackson Lab., Bar Harbour, MA) mice were housed in a HEPA-filtered air environment. All experiments were conducted with mice between 8 to 10 weeks

of age in compliance with the regulations of the Animal Committee of the University of Quebec in Montreal (CIPA).

Viruses

MHV3 is a cloned pathogenic substrain isolated from the liver of infected DBA2 mice. The MHV3 virus induces a rapid mortality in C57BL/6 mice within 3 to 4 days post infection (p.i.) (23). The escape mutant 51·6-MHV3 was selected from the pathogenic MHV3 virus cultured into L2 cells in the presence of S protein-specific A51 monoclonal antibodies (24). This variant induces a delayed mortality (5 to 9 days p.i.) and expresses low tropism for LSECs but retains ability to infect Kupffer cells (KC) (24). The non-pathogenic YAC-MHV3 variant is a cloned substrain produced in persistently infected YAC-1 cells, showing lower ability to replicate in LSECs and macrophages. Compared to the attenuated 51.6-MHV3 strain, this variant causes no mortality and induces efficient recruitment of innate immune cells allowing viral clearance from the liver within two weeks p.i. (31). All viruses were passaged less than three times onto L2 cells and their pathogenic properties were assessed routinely.

Isolation and purification of LSECs

Mice were euthanized and the portal vein was isolated and injected with 3 mL of HBSS 10nM HEPES followed by 3mL of digestion buffer consisting of 0.2% (w/v) collagenase A in HBSS 10nM HEPES (Sigma Aldrich, St-Louis, MO). The liver was then excised, injected several times with digestion buffer and dissociated by a 30 min incubation in 10 ml of

digestion buffer at 37°C on a shaking plate (200 RPM). The resulting cell suspension was passed through a sterile 70uM and a 40uM nylon mesh filter successively (Falcon, BD Biosciences, Mississauga, Ont., Canada) and centrifuged at 400*g* for 10 min. Cell pellet was resuspended in 3ml of RPMI 1640, layered at the top of a discontinuous 50%/25% Percoll gradient (Sigma Aldrich) and centrifuged at 800*g* for 20 min without brakes. The interphase between the two density cushions, containing enriched non-parenchymal cells, was collected and washed with PBS. LSEC were then purified using the positive selection PE kit (Stemcell, Vancouver, Canada) with an anti-CD146 monoclonal antibody, a specific marker of endothelial cells in liver (33), according to the manufacturer's procedure. LSEC purity was analyzed by cytometry before each experiment and reached over 90%.

In vivo viral infections

Groups of 6-7 wild type C57BL/6 or TLR2 KO mice were intraperitoneally infected with 10^3 TCID50 of MHV3, 51.6-MHV3 and/or YAC-MHV3. Mock-infected mice received a similar volume of PBS (Wysent). Mice were sacrificed by CO_2 anoxia at 24, 48 and/or 72 h postinfection (p.i.) according to experiment. Liver and blood were collected and frozen for further analyses.

Histopathological, transaminase levels and immunohistochemical analyses

The histopathological analysis of liver was done by hematoxylin-eosin-safranine staining. Determination of serum ALT and AST transaminases was performed according to the IFCC primary reference procedures using Olympus AU2700 Autoanalyser® (Olympus Optical,

Tokyo, Japan). Immunolocalization of IL-33 and CAV-1 was performed on liver sections fixed in paraformaldehyde and embedded in paraffin incubated with primary goat anti-mouse IL-33 (R&D System Inc., Minneapolis, MN) or rabbit anti-mouse-CAV-1 (LSBio, Seattle, WA) for 1h in Ventana automated machine (Ventana Medical Systems, Inc. Tucson, AZ) and secondary HRP-conjugated rabbit anti-goat antibody (Dako, Markham, ON, Canada) or OmniMap anti-Rabbit-HRP (RUO) for 16 min. Double immunofluorescence stainings of IL-10 or IL-33 and CAV-1 were conducted on liver cryosections fixed in paraformaldehyde and incubated overnight with primary goat anti-mouse IL-10 (R&D System Inc., Minneapolis, MN) or primary goat anti-mouse IL-33 (R&D System) and rabbit anti-mouse-CAV-1 (LSBio) and then with DyLight-649-Anti goat Cy3-Anti Rabbit (Jackson ImmunoResearch, West Grove, PA) secondary antibodies and Hoechst counterstain (Invitrogen, Ontario, Canada). Slides were mounted (mounting medium, Invitrogen, Ontario, Canada), imaged with a Nikon's Eclipse Ni-E Z1 microscope and analyzed using SpotAdvance software.

Virus titration

Frozen liver samples from 24 and/or 72 h MHV-infected mice were weighted and homogenized in cold PBS. Suspension was then centrifuged at 13000 RPM for 30 min and analyzed for viral detection. Viral titration was also performed on LSEC culture supernatants. Liver suspension and cell culture supernatants were 10-fold serial-diluted and tested for viral presence on L2 cells cultured in 96-well plates. Cytopathic effects (CPE), characterized by occurrence of large syncytia and cell lysis, were recorded at 72 h p.i. and

227 virus titers were determined according to Reed-Muench method and expressed as $\log_{10}$
228 tissue culture infectious dose $(TCID)_{50}$.
229
230 ***In vitro viral infections***
231 Freshly isolated LSEC were seeded in 24-well plates at a density of 7,5 x 10^5 cells/ ml in
232 RPMI 1640 supplemented with 10% fetal calf serum (FCS) and antibiotics (Wysent, St-
233 Bruno, Qc, Canada). Cells were then infected with 0.1 multiplicity of infection (MOI) of
234 infectious MHV3, YAC-MHV3 or 51.6-MHV3 and incubated at 37°C, under 5% CO_2 for 24
235 to 72 h according to experiment. Cell culture supernatants were collected for ELISA assays
236 and total RNA was extracted for qRT-PCR analysis.
237
238 ***siRNA transfection***
239 LSECs were seeded in 24-well plates at 60 000 cells/ml and transfected with 25 nM of
240 siRNA Flexitude premix (Qiagen, Cambridge, MA) targeting TLR2 mRNA (target
241 sequence: CTCGTTCTCCAGCATTTAAA) and with the AllStars Negative Control siRNA
242 as nonsilencing transfection control for 36 h prior to infection for 24 h**.**
243
244 ***RNA isolation and RT-qPCR***
245 RNA from *in vitro* infected LSEC was extracted using NucleoSpin RNA II kit (Macherey-
246 Nagel, Bethlehem, PA) according to the manufacturer procedure. Total RNA from frozen
247 liver samples was extracted using TRIzol reagent (InVitrogen, Burlington, ON, Canada) and
248 residual genomic DNA was removed with the Turbo DNA-free kit (Ambion, Austin, TX).

One µg of RNA was retro-transcribed into cDNA using the High capacity cDNA reverse transcription kit (Applied Biosystems, Foster City, CA). Real time PCR amplification was carried out on 25ng cDNA using the HotStart-IT™ SYBR® Green qPCR Master Mix (USB Corporation, Cleveland, OH) on a ABI 7300 system (Applied Biosystems). Primer sets used are listed in Table I. Threshold cycle values (Ct) were collected and used for "ΔΔCt" analysis. The relative gene expression was normalized to HPRT as endogenous control and expressed as a ratio to gene expression in mock-infected mice livers or control (uninfected) LSECs in *in vitro* experiments (level arbitrarily taken as 1). The specificity of the PCR products was confirmed by melting curve analyses and all qPCR assays were run in duplicate.

ELISA and nitric oxyde assays

Frozen liver samples were weighted and homogenized in NP40 lysis buffer (InVitrogen) completed with a protease inhibitor cocktail (Sigma Aldrich, St-Louis, MA) and 1 mM PMSF for protein extraction. Liver suspension was kept on ice for 30 min and centrifuged 10 min at 13000 RPM. Determination of IL-6, TNF-α (BD BioSciences, San Jose, CA) CXCL10, CCL2 (eBiosciences, San Diego, CA), CXCL1 and IL-33 (R&D Systems, Minneapolis, MN) in liver lysates and/or LSEC culture supernatants was carried out by ELISA tests. Levels of nitric oxide (NO) were quantified using the Griess reagent assay (InVitrogen) according to the manufacturer's procedure.

Cytofluorometric studies

Livers were perfused with PBS through the portal vein to remove blood cell contamination prior to dissection. Liver tissues were then homogenized and hepatocytes were removed by sedimentation. Inflammatory cells were enriched using 35% Percoll gradient (Sigma Aldrich) and red blood cells were lyzed with a Tris-buffered ammonium chloride solution. A million ($10^{6)}$ of leucocytes were incubated with anti-CD16/32 antibodies (BD Biosciences) to block non-specific binding. Cells were incubated with optimal dilutions of anti-CD3-V500, anti-Gr1-V450, anti-CD11b-PE-Cy7, anti-CD19-APC, anti-CD4-FITC, anti-NK1.1-PerCP-Cy-5.5 and anti-CD8-APC-Cy7 antibodies (BD Biosciences) and fixed in PBS containing 2% FCS, 0.01 M sodium azide and 2% formaldehyde. Stained cells were analyzed on a FACS Aria II ® flow cytometer using BD FACS Diva software (BD Bioscience) and the data were processed using CXP software (Beckman Coulter, Mississauga, ON, Canada). Dead cells and doublet cells were excluded on the basis of forward and side scatter and analyses were performed on 10,000 events recorded. Myeloid cells, gated by high side scatter, were assessed for CD11b and Gr1 to enumerate macrophages ($CD11b+Gr1^{inter}$) and neutrophils ($CD11b^{+}Gr1^{high}$). Lymphoid cells were gated according to FSC/SCC and first assessed for NK1.1 and CD3 expression to discriminate NK from NKT cells. CD3+NK1.1- T cells were further gated to allow determination of CD4+ and CD8+ subpopulations. B lymphocytes were determined by CD19+ CD3- expression.

Statistical analyses

Data are expressed as means ± the standard error of the mean. Statistical analyses for *in vitro* studies were performed with Student's t-test comparing uninfected (control) to virus-infected cells or virulent to attenuated MHV3 infections. Multiple group analyses were conducted for *in vivo* studies and data obtained by qPCR, ELISA and viral titration were evaluated by one-way ANOVA test with *posthoc* Tukey test using PASW Statistics software (PASW version 18, IBM SPSS Inc. Chicago, IL). Values of $p \leq 0.05$ were considered as significant.

RESULTS

Lower tropism of attenuated MHV3 variants for LSECs is associated with less severe damages and viral replication in the liver

Previous studies have shown that acute infections by the attenuated 51.6- and YAC-MHV3 variants resulted in milder or subclinical hepatitis respectively in comparison to fulminant hepatitis induced by the parental virulent MHV3 strain (24, 31). We first aimed to compare the evolution of damages, inflammatory infiltrates and viral replication in the liver of mice infected by virulent and attenuated MHV3 strains. C57BL/6 mice were i.p. infected with either MHV3 or attenuated viruses for 24 to 72 h p.i., and blood and livers were collected for clinical, histopathology and viral titer analyses. Liver histopathology from virulent MHV3-infected mice showed inflammatory foci surrounding necrotic cells at 24 h and 48 h p.i. which disappeared at 72 h p.i. while hepatocyte necrosis became extensive (Fig. 1 A and B).

Infection with 51.6-MHV3 revealed delayed occurence of inflammatory foci at 48 h p.i. with barely detectable hepatic damages while YAC-MHV3 induced few small inflammatory infiltrates with no observable hepatic necrosis areas even at 72 h p.i. (Fig. 1 A and B). Extensive hepatic damages in virulent MHV3-infected mice correlated with high levels of blood ALT and AST transaminases at 72 h p.i. ($p \leq 0.001$) (Fig. 1 C and D) and sooner and higher viral replication than in attenuated 51.6-and YAC-MHV3 variants-infected mice ($p \leq 0.01$ to 0.001) (Fig. 1 E and F).

Attenuated MHV3 strains induce lower Fgl-2, CAV-1 and IL-33 expression in the liver than virulent MHV3

Vascular and structural disorders in LSECs were reported in viral hepatitis, correlating with hepatic damages (19, 27, 29). Indeed, previous studies have demonstrated that induction of Fgl-2, a prothrombinase expressed by LSECs promoting vascular thrombosis and hepatic inflammation, correlated with MHV3-induced fulminant hepatitis (28). Moreover, a direct association between capillarization (lack of fenestrations) of LSECs in livers from HCV-infected patients and an overexpression of caveolin-1 (CAV-1), a key component of LSECs fenestrations, was recently evidenced (34). To verify whether the lower severity of hepatitis induced by the attenuated MHV3 strains was associated with lower dysfunctions in LSECs, mRNA levels for CAV-1 and Fgl2 were quantified by qRT-PCR in livers from all infected groups of mice. Intrahepatic expression of CAV-1 was also localized by immunohistochemistry staining in MHV3- and 51.6-MHV3-infected mice. As shown in

figure 2A, higher increase of CAV-1 mRNA levels were observed at 48 h p.i. in the liver of MHV3-infected mice while lower or no induction was noted in 51.6- and YAC-MHV3-infected mice, respectively ($p \leq 0.05$ and 0.001). Immunolocalization of CAV-1 revealed specific expression in LSECs and confirmed higher induction in the liver of MHV3- than 51.6-MHV3-infected mice (see black arrow, Fig. 2B). Gene expression of Fgl2 increased as soon as 24 h p.i. in mice infected with MHV3 while it was delayed and lower in 51.6-MHV3 infection or not induced in YAC-MHV3-infected mice ($p \leq 0.05$ to 0.001) (Fig. 2C). In addition, Fgl-2 mRNA reached higher levels in the liver of virulent than attenuated MHV3-infected mice ($p \leq 0.001$).

We have recently reported that MHV3 infection was associated with early release of IL-33, an alarmin mainly secreted by injured LSECs (29). We aimed to verify whether lower tropism of attenuated MHV3 strains for LSECs may be associated with lower expression of IL-33. To test this hypothesis, mRNA expression, production and localization of IL-33 were assessed by qRT-PCR, ELISA and IHC, respectively, in livers from MHV3 and 51.6-MHV3 infected groups of mice. As shown in figures 2D and E, gene expression and release of IL-33 increased only in the liver of MHV3-infected mice ($p \leq 0.001$) while it was rather not induced or inhibited in mice infected with 51.6- or YAC-MHV3 ($p \leq 0.05$ to 0.01). IHC stainings indicate that expression of IL-33 was only induced in the liver of MHV3-infected mice and mostly localized in LSECs, and at a lesser extent in hepatocytes nuclei (Fig. 2F). Induction of IL-33 in LSECs was confirmed by a double immunostaining IL-33/caveolin-1 in livers from MHV3-infected mice at 48 h p.i. and to a lesser extent at 72 h p.i. (Fig. 2G).

359

360 *Virulent MHV3 infection leads to an imbalance of pro- over anti-inflammatory mediators in*
361 *the liver in contrast to infection by attenuated MHV3 strains*

362

363 Given the crucial role of LSECs in the control of liver inflammation through production of
364 anti-inflammatory cytokines, we presumed that dysfunctions of LSECs in MHV3-infected
365 mice may favor the induction of a pro-inflammatory state in the liver. To verify this
366 hypothesis, levels of anti-inflammatory cytokines (IL-10, TGF-β) and proinflammatory
367 cytokines (IL-6, TNF-α) and chemokines (CCL2, CXCL1, CXCL10) were assayed by qRT-
368 PCR (from 24 to 72 h p.i.) and ELISA (72 h p.i.) in the liver of all groups of infected mice.
369 As indicated in the figure 3 sect.I A and B, mRNA expression levels and production of IL-
370 10 were markedly increased in the liver of 51.6-MHV3- and YAC-MHV3-infected mice
371 when compared to lower levels induced in MHV3-infected mice ($p \leq 0.05$ to 0.001). At a
372 lesser extent, TGF-β mRNA and production levels were also higher induced in the liver of
373 51.6-MHV3-infected mice, especially at 24 and 48 h p.i. ($p \leq 0.05$ to 0.001)(Fig. 3 C-D). To
374 verify whether IL-10 induction in the liver of 51.6-MHV3-infected mice occurred in
375 endothelial cells (EC), immunohistochemistry stainings using specific antibodies to IL-10
376 and CAV-1 (EC marker) were conducted on liver sections. In comparison to staining in
377 mock-infected mice, IL-10 expression in livers from 51.6-MHV3-infected mice was induced
378 in the parenchyma and in venous and sinusoidal ECs whereas occurrence and intensity of
379 IL-10 staining were weaker in MHV3-infected mice (Fig.3 sect. II)

380

On the other hand, mRNA expression and production levels of intrahepatic IL-6 and TNF-alpha were higher up-regulated in MHV3- than 51.6- or YAC-MHV3-infected mice ($p \leq 0.05$ to 0.001) (Fig. 3 sect.I E-H). In the same line, transcription and production levels of the chemokines CXCL1, CCL2 and CXCL10 increased throughout infection by MHV3 but were delayed or dramatically reduced in 51.6- or YAC-MHV3-infected mice ($p \leq 0.05$ to 0.001) (Fig. 3 sect.III A-F).

Virulent MHV3 induces higher expression of TLRs and helicases in the liver than attenuated MHV3 strains

Induction of inflammatory response during viral infection is triggered upon activation of PRRs, such as TLRs and helicases, by viral products. Several studies have reported increased TLR expression in viral hepatitis, correlating with liver inflammation (reviewed in 17). We explored the hypothesis that higher release of inflammatory mediators in MHV3 infection may be related to increased expression of TLRs or helicases in the liver. Thus, the kinetics of surface TLR-2 and -4, endosomal TLR-3 and -7, and helicase RIG-1 and MDA-5 gene expression were compared by qRT-PCR in the liver of infected mice from 24 to 72 h p.i. As shown in figure 4A, TLR2 expression steadily higher increased over the course of infection with MHV3 while its induction was drastically reduced in mice infected with the attenuated variants ($p \leq 0.01$ to 0.001). Expression levels of TLR3, TLR4, RIG-1 or MDA-5 genes were only or more increased during MHV3 than in 51.6- or YAC-MHV3 infections

albeit markedly lesser than TLR2 ($p \leq 0.05$ to 0.001) (Fig. 4B, C, E and F), whereas levels of TLR7 were unaffected by neither viruses (Fig. 4D).

These data suggest that higher levels of inflammatory mediators in the liver of MHV3-infected mice may be associated with preferential and higher induction of PRRs, especially TLR2, by the virulent MHV3.

Hepatic proinflammatory state in virulent MHV3-infected mice leads to rapid but transient intrahepatic recruitment of inflammatory cells and decrease of B,CD4 and CD8 lymphocyte subsets

LSECs are responsible for the recruitment and transmigration of leucocytes during liver inflammation (35). We postulated that higher production of chemokines in the liver of MHV3-infected mice induced higher recruitment of inflammatory cells than in mice infected with attenuated virus strains. Such hypothesis was supported by higher occurrence of inflammatory infiltrates in the liver of MHV3-infected mice at 24h p.i. (see Fig. 1A). To determine leukocyte subsets recruited into the liver, intrahepatic mononuclear cells were isolated at 24 and 48 h p.i. from all groups of mice, immunolabeled, and the percentages of NK-T (NK1.1+CD3+) and NK (NK1.1+CD3-) cells, neutrophils ($CD11b^{hi}Gr1^{hi}$), macrophages ($CD11b^{+}Gr1^{int}$), B (CD19+) and T (CD8+ and CD4+) cells were analyzed by cytometry and compared to cells from mock-infected mice. As shown in figure 5, section I-A , percentages of NK-T cells transiently decreased in the liver of MHV3-infected mice ($p \leq$

424 0.001) differing to that seen livers from 51.6- and YAC-MHV3 infected mice ($p \leq 0.05$ to
425 0.01). NK cell percentages higher increased in MHV3- than 51.6-MHV3-infected mice
426 while it decreased in YAC-MHV3 ($p \leq 0.05$ to 0.001) (Fig. 5, section I-B). Neutrophils,
427 however, were earlier and higher recruited into the liver of MHV3- than in 51.6- and YAC-
428 MHV3-infected mice ($p \leq 0.05$ and 0.001) (Fig. 5, section I-C). Percentages of intrahepatic
429 macrophages more increased in MHV3-infected mice ($p \leq 0.05$ to 0.001) (Fig. 5 , section I-
430 D). Regarding lymphocyte subsets, B and CD4+ cell percentages stronger decreased in the
431 liver of MHV3-infected mice ($p \leq 0.05$ and 0.001)(Fig.5, section I-E-F) while CD8+ cells
432 were higher reduced by 51.6- or YAC-MHV3 infections ($p \leq 0.05$ to 0.001) (Fig.5 , section
433 I-G).
434
435 Since a substantial decrease in total number of isolated intrahepatic cells was noted over
436 infection time with MHV3 only, the analysis of absolute numbers of each cell subset rather
437 than the relative percentages better reflects the recruitment of inflammatory cells. Cell
438 numbers were then determined, using the percentage of each subset reported to total number
439 of isolated cells in the liver of each mice. As shown in figures 5, section II-A and B, NK-T
440 cells decreased only in the liver of MHV3-infected mice ($p \leq 0.01$ and 0.001) while total NK
441 cells were not altered in all infected groups. Number of neutrophils, however, earlier but
442 transiently increased at 24 h p.i. in MHV3-infected mice while they were delayed or lower
443 recruited in livers from 51.6- and YAC-MHV3-infected mice respectively when compared
444 to MHV3 infection ($p \leq 0.05$ to 0.001) (Fig. 5, section II-C). In contrast to that observed
445 with percentages, numbers of intrahepatic macrophages increased in the liver of mice

446 infected with attenuated YAC- and 51.6-MHV3 strains ($p \leq 0.01$ and 0.001) but not with
447 MHV3, but such increases were not statistically significant when compared to MHV3
448 infection (Fig. 5, section II-D). The numbers of B and T (CD4 and CD8) cells were also
449 dramatically impaired over the course of infection by MHV3, but were less or not altered by
450 51.6- or YAC-MHV3 infections or transiently increased at 24 h p.i. in YAC-MHV3-infected
451 mice ($p \leq 0.05$ to 0.001) (Fig. 5, section II- E andG).
452
453 *Permissivity of LSECs to MHV3 strains correlates with virulence.*
454
455 We next attempted to characterize the effect of virulent and attenuated MHV3 infection on
456 functional and structural integrity of LSECs *in vitro*. LSECs were isolated from the liver of
457 C57BL/6 mice and purified by Percoll gradient followed by immunomagnetism using the
458 anti-CD146 antibodies. As shown in the figure 6A, 87 to 91% of isolated cells expressed the
459 endothelial markers CD146, CD54 (ICAM-1), and CD31 (PECAM-1) but not the
460 macrophage marker F4/80. Isolated LSECs were then infected by the MHV3 strains and
461 viral replication as well as CPE were monitored from 24 to 120 h p.i. CPE in LSECs was
462 characterized by cell lysis and rounded shaped cells instead of typical MHV-induced giant
463 syncytial cells (usually observed in L2 cells) and occurred sooner in virulent MHV3-infected
464 culture as cells were totally lysed by 72 h p.i. In contrast, CPE in cells infected by attenuated
465 strains were delayed to 72 h p.i. and increased up to 120 h p.i. (Fig.6B) ($p \leq 0.001$ when
466 compared with MHV3-infected cells). Infectious viruses in supernatants from MHV3-
467 infected LSECs were detected at 48 h p.i and then started to decrease as cell damages

468 became extensive whereas titers of 51.6- and YAC-MHV3 were only detected after 96 or
469 120 h p.i. (Fig. 6C) ($p \leq 0.001$ when compared with MHV3-infected cells).
470
471 *Virulent but not attenuated MHV3 strain induces Fgl2, IL-33 and caveolin-1 expression and*
472 *alters NO production by LSECs*
473
474 To confirm that attenuated MHV3 variants, in contrast to MHV3 virus, do not disturb
475 LSECs integrity and vascular factors, as observed in vivo, expression level of the alarmin
476 IL-33 and the prothrombinase Fgl-2 were evaluated respectively in infected LSECs. As
477 expected and shown in the figures 7A to C, gene expression and release of IL-33 increased
478 throughout infection only in MHV3-infected cells ($p \leq 0.05$ to 0.001) while Fgl2 expression
479 was up-regulated at 48 h p.i. in MHV3-infected cells only ($p \leq 0.05$ to 0.001). Lower levels of
480 Fgl2 mRNA at 72 h p.i. ($p \leq 0.05$) reflected total cell lysis in MHV3-infected LSECs.
481
482 MHV3 replication was already shown to be controlled *in vitro* by nitric oxide (NO) (36).
483 Since LSECs constitutively release NO, a vasodilatator factor regulating sinusoidal blood
484 flow (37), we verified whether higher replication of MHV3 in LSECs may result from defect
485 in NO production by quantifying NO levels in culture supernatants. As shown in figure 7D,
486 release of NO was reduced only in MHV3-infected cells differing thus with 51.6-MHV3- or
487 YAC-MHV3-infected cells ($p \leq 0.01$) (Fig. 7B). Since NO production was reported to be
488 negatively regulated by CAV-1 through inhibition of endothelial nitric oxide synthase
489 (eNOS) activity (38), we investigated whether NO alteration by MHV3 infection was

490 associated with up-regulation of CAV-1 expression in infected LSECs, as seen in the liver of
491 MHV3-infected mice. In agreement with our *in vivo* observations, mRNA expression level
492 of CAV-1 increased only in MHV3-infected LSECs at 24 and 48 h p.i. (fig. 7E) ($p \leq 0.05$ to
493 0.001).
494
495 *Virulent MHV3, in constrast to attenuated strains, promotes LSECs conversion into a*
496 *proinflammatory profile*
497
498 MHV3-infected mice exhibited higher inflammatory response in the liver than mice infected
499 by attenuated strains, suggesting defect in the control of inflammation by LSECs. LSECs
500 were already reported to produce IL-6 upon infection by MCMV (5), indicating a possible
501 switch from an anti- to pro-inflammatory phenotype once infected. We thus speculated that
502 LSECs infected by MHV3, in comparison to attenuated strains, may adopt a preponderant
503 proinflammatory profile. To address this, mRNA expression and production levels of anti-
504 inflammatory (IL-10 and TGF-β) and proinflammatory (IL-6, TNF-α) cytokines produced
505 by infected LSECs were determined by qRT-PCR and ELISA assays. As shown in Fig. 8
506 section I-A and B, mRNA expression and production of IL-10 slightly increased at 24 h p.i.
507 in MHV3-infected LSECs but decreased thereafter below the basal level in uninfected cells
508 ($p \leq 0.05$ and 0.001). Consistent with the up-regulation of IL-10 in the liver of mice infected
509 with attenuated MHV3 strains, IL-10 levels rapidly or progressively higher increased in
510 51.6-MHV3- and YAC-MHV3- than in MHV3-infected LSECs up to 72 h p.i. ($p \leq 0.05$ to
511 0.001). TGF-β expression, however, was not or slightly induced in cells infected by the

attenuated strains ($p \leq 0.05$) but was less inhibited in attenuated virally-infected cells than in virulent MHV3-infected cells ($p \leq 0.05$ and 0.01) (Fig. 8 section I-C and D). These results suggest that MHV3 infection suppresses anti-inflammatory function of LSECs whereas attenuated strains rather promote it.

TNF-α mRNA levels, however, rather transiently increased only in MHV3-infected LSECs at 24 h p.i. ($p \leq 0.01$) (Fig. 3 section. I-E) and were completely inhibited at 72 h p.i. by all MHV3 strains ($p \leq 0.01$). Amounts of TNF-α released in supernatants of infected LSECs, however, increased in all infected cells ($p \leq 0.001$) but remained higher in MHV3 and YAC-MHV3- than 51.6-MHV3-infected cells ($p \leq 0.05$) (Fig. 8 section I-F). The mRNA expression of IL-6 reached higher levels in cells infected by virulent MHV3 than attenuated strains at 24 h p.i. only ($p \leq 0.05$ to 0.001) (Fig. 8 section I-G), correlating with higher release in supernatant of MHV3-infected cells ($p \leq 0.01$) (Fig. 8 section I-H).

LSECs were also reported to secrete chemokines upon infection by Dengue virus and to enchance their production in chronic inflammatory liver disease (39, 40). Thus, we presumed that MHV3-infected LSECs may produce higher levels of chemokines. As shown in figure 3, section II-A to D, CXCL1 and CCL2 expressions were higher upregulated in MHV3-infected LSECs than in 51.6- and YAC-MHV3-infected cells at 24 and 48 h p.i. leading to higher amounts released in cell supernatants ($p \leq 0.05$ to 0.001). CXCL10 gene expression and production levels only increased in MHV3-infected LSECs ($p \leq 0.05$ to 0.001) (Fig. 8 section II- E and F).

534

535 *Proinflammatory activation of LSECs by MHV3 depends on TLR2 signalling*

536

537 We have previously shown that induction of inflammatory cytokines by MHV3 in *in vitro*
538 infected macrophages depended on TLR2 signaling (37). In addition, Liu et al. (9) recently
539 demonstrated that TLR2 activation on LSECs reversed their anti-inflammatory functions.
540 Since TLR2 was strongly up-regulated in livers from MHV3-infected mice, we aimed to
541 investigate whether TLR2 was involved in the conversion of LSEC towards a
542 proinflammatory profile. We first sought to determine whether MHV3 increased TLR2
543 expression on LSECs. As shown in figure 9A, levels of TLR2 mRNAs were significantly
544 higher in cells infected by MHV3 than attenuated strains at 24 h p.i. ($p \leq 0.05$ to 0.01). To
545 address whether TLR2 was involved in cytokine response and viral replication in infected
546 LSECs, TLR2 expression was abrogated by siRNAs prior to infection and IL-6 and CXCL1
547 mRNA levels were determined by qRT-PCR at 24h p.i. Viral replication of MHV3, but not
548 51.6 and YAC-MHV3, was significantly reduced following TLR2 knockdown ($p \leq 0.001$)
549 (Fig. 9B). A markedly decreased expression of IL-6 and CXCL1 and an up-regulation of IL-
550 10 levels were also observed in MHV3-infected cells rendered defective for TLR2 while no
551 difference was noted in cells infected with the attenuated variants ($p \leq 0.001$)(Fig. 9C to E)
552 ($p \leq 0.001$). These results suggest that higher tropism and pro-inflammatory inducible
553 capacities of MHV3 in LSECs reflect its unique ability to activate TLR2 signalling.

554

555 *TLR2 exacerbates liver damage and increases viral replication in mice infected by virulent*
556 *but not attenuated MHV3 strains*
557
558 We already reported that MHV3-induced acute hepatitis was less severe in TLR2 KO mice
559 (41). To verify whether TLR2 is differentially involved in the evolution of hepatitis induced
560 by virulent and attenuated MHV3 strains, groups of wild type (WT) C57BL/6 and TLR2
561 knock-out (KO) mice were i.p. infected with MHV3 or 51.6-MHV3. Survival rate was
562 monitored and liver damage and viral load were evaluated at 72 h p.i. As shown in figure
563 10A and B, survival of TLR2 KO mice infected by MHV3, but not 51.6-MHV3, was
564 prolonged when compared to respective infected WT mice ($p \leq 0.001$). Accordingly,
565 histopathological analysis of the liver revealed less and smaller necrotic foci in MHV3-
566 infected TLR2 KO mice than in WT mice whereas comparable and barely detectable hepatic
567 damages were noted in TLR2 KO and WT mice infected with 51.6-MHV3 (Fig. 10C).
568
569 In addition, viral replication of MHV3 at 72h p.i. was lower in the liver of infected TLR2
570 KO than WT mice whereas 51.6-MHV3 replication was similar in both mice strains (Fig.
571 10D) ($p \leq 0.001$). Taken together, these results suggest that TLR2 aggravates hepatic
572 damages and viral replication in mice infected by virulent but not attenuated MHV3 strains.
573
574 *TLR2 activation by virulent MHV3 decreases IL-10 and increases inflammatory cytokines*
575 *and chemokines expression*
576

577 It was previously reported that hepatic levels of IL-6 and TNF-α were reduced in MHV3-
578 infected TLR2 KO in comparison to C57BL/6 mice, suggesting a role for TLR2 in MHV3-
579 induced release of inflammatory factors (41). Thus, we speculated that MHV3, in contrast to
580 51.6-MHV3, may promote a pro-inflammatory cytokine profile in the liver through TLR2
581 activation, such as observed in *in vitro* infected LSECs. To test this hypothesis, expression
582 levels of several inflammatory and anti-inflammatory factors were compared between livers
583 from TLR2 KO and wild type (WT) mice infected with both viruses. As shown in Table II,
584 lower mRNA expression of TNF−α, IL-6, CXCL1, CCL2, CXCL10 and higher IL-10 levels
585 occurred in the liver of MHV3-infected TLR2 KO mice compared to WT mice ($p \leq 0.001$)
586 whereas levels of Fgl2 and IL-33 were similar in both mouse strains. In contrast, no
587 difference was observed between cytokine profile in 51.6-MHV3-infected WT and TLR2
588 KO mice, albeit a slight reduction of CXCL10 expression was noted in TLR2 KO mice ($p \leq$
589 0.05). Given the importance of IL-10 in the control of hepatic inflammation, we aimed to
590 determine whether higher levels in livers from MHV3-infected TLR2 KO mice reflected
591 higher production by ECs. A double immunohistochemistry staining of IL-10 and CAV-1 on
592 liver sections revealed that expression of IL-10 in ECs was effectively higher in livers from
593 MHV3-infected TLR2 KO than WT mice (Fig. 11 compared with Fig. 3 section II).
594
595 **DISCUSSION**
596
597 In this work, we investigated the role of LSECs in hepatic inflammation during acute viral
598 hepatitis process using the MHV3 model of infection. We demonstrated that the severity of

599 hepatitis, viral replication and hepatic inflammation correlated with permissivity of LSECs
600 for MHV3 strains and subsequent structural and functional disturbances. We showed that *in*
601 *vitro* infection of LSECs by the virulent MHV3, in contrast to the attenuated 51.6- and
602 YAC-MHV3 variants, resulted in earlier cell damage and disorders in inflammatory and
603 vascular factors, as reflected by high release of inflammatory cytokines/chemokines and pro-
604 coagulant Fgl-2 and a decrease in NO and IL-10 levels. We evidenced that the higher
605 replication rate and proinflammatory activity of MHV3 in LSECs was associated with its
606 specific activation of TLR2 signalling in LSECs and exposed that TLR2 is a key factor of
607 hepatic inflammation and LSEC-derived IL-10 disorders in MHV3-induced fulminant
608 hepatitis.
609
610 LSECs, lining the hepatic sinusoids, mediate liver tolerance under physiological conditions
611 (reviewed in 1) but these cells are target of many hepatotropic viruses. The consequence of
612 LSECs infection in inflammatory liver diseases such as viral hepatitis has never been
613 investigated. We have shown that MHV3 infection induced differential structural and
614 functional disorders in LSECs according to strain virulence. Indeed, the highly virulent
615 MHV3 replicated faster and higher in LSECs leading to occurrence of CPE such as change
616 in morphology (rounded cells) and cell lysis from 48 h p.i. Previous reports have already
617 shown that *in vivo* and *in vitro* infections of LSECs by MHV3 were associated with cell
618 damages and loss of fenestrations (27), but no syncytial cells were observed. However,
619 MHV3 did not replicate in LSECs as fast as it usually does in *in vitro* cultured cells since no
620 viral burden was detected until 48 h p.i. while MHV3 titers are detectable within 24 h p.i. in

621 macrophages (24, 41). Our results are nevertheless in accordance with those from Pereira et
622 al. (26) who have shown that MHV3 replicates more rapidly in Kupffer cells (KC cells) than
623 in LSECs *in vitro*, suggesting that LSECs may transiently control the viral replication.

624 In agreement, replication of the attenuated 51.6- and YAC-MHV3 variants was delayed to
625 96 or 120 h p.i. and was associated with barely detectable CPE, reflecting their weaker
626 tropism for LSECs. It was recently reported that LSECs exhibit high clearance capacity of
627 circulating viruses (42, 43), suggesting that they may express high ability to sequester
628 attenuated but not virulent MHV3 particles. However, as replication of MHV3 variants in
629 LSECs was delayed but not aborted rather suggests a host cell-dependent control mechanism
630 of viral replication. Indeed, preliminary results showed higher antiviral IFN-β response in
631 LSECs infected by attenuated MHV3 strains (results not shown). The low IFN-β response in
632 virulent MHV3-infected LSECs may be related to specific viral evasion mechanisms from
633 host viral sensors or interference with downstream signaling pathways. We have observed
634 that MHV3, in contrast to attenuated strains, neither induced TLR3 nor RIG-I expression in
635 LSECs (results not shown), suggesting lower detection by these viral sensors. Further work
636 should address whether viral products or evasion strategies are involved in MHV3-induced
637 impairment of IFN-β response in LSECs.

638

639 The inability of attenuated MHV3 variants to establish a rapid infection in LSECs correlated
640 with a less severe hepatitis. Indeed, 51.6-MHV3 infection resulted in lower viral replication,
641 transaminase levels and liver damages than MHV3 infection. The 51.6-MHV3 variant only

642 differs from the pathogenic MHV3 by its weaker tropism for LSECs but retained its
643 virulence for hepatocytes, KCs and Ito cells (24), suggesting that resistance of LSECs to
644 viral replication may protect against fulminant hepatitis. Similarly, the non pathogenic
645 YAC-MHV3, also expressing low ability to replicate in LSECs, induced light and transient
646 hepatic lesions, reinforcing the importance of functional integrity of LSECs in the evolution
647 of viral hepatitis. Indeed, less severe hepatic damages and viral load in mice infected with
648 the attenuated variants may possibly result from a better early control of viral replication by
649 LSECs leading to reduced transmission of viral progeny to the hepatic parenchyma. In
650 agreement, a delayed replication of MHV3 in LSECs was suggested as a crucial step in the
651 resistance of various strains of mice to MHV3 infection by allowing time for the local and
652 systemic responses to clear the infective particles (26).
653
654 We report here for the first time that *in vitro* MHV3 infection promotes a proinflammatory
655 activation of LSECs. Indeed, MHV3 induced higher levels of IL-6, TNF-α and chemokines
656 in LSECs than attenuated strains and inhibited their basal release of IL-10 while attenuated
657 strains rather enhanced it. These inflammatory disorders in LSECs correlated with higher
658 ratios of intrahepatic inflammatory over anti-inflammatory mediators in the liver of MHV3-
659 infected mice, suggesting that LSECs may have lost their ability to control inflammation. In
660 agreement, IL-10 staining was significantly lower in ECs from the liver of mice infected by
661 MHV3 than by attenuated strains. The importance of IL-10 production by LSECs in the
662 suppression of pro-inflammatory cytokine release by Th1 and Th17 was recently evidenced
663 by Carambia et al. (44). In addition, LSECs were recently shown to be more efficient than

664 KCs in tolerizing autoreactive Th1 cells via IL-10 (2). The lower inflammatory profiles in
665 livers from 51.6- and YAC-MHV3-infected mice are in line with our previous observations
666 (30). The highly attenuated YAC-MHV3 infection correlated with lower induction of
667 inflammatory mediators than 51.6-MHV3 infection. Higher levels of anti-inflammatory IL-
668 10 and immunosuppressive PGE2 were already reported in the liver of YAC-MHV3- than
669 51.6-MHV3-infected mice (30), suggesting that the highly attenuated phenotype of YAC-
670 MHV3 may reflect the preservation of integrity of LSECs and other yet unindentified
671 hepatic cells. Since YAC-MHV3, unlike 51.6-MHV3, was shown to lower replicate in
672 macrophages *in vitro* (45), it is plausible that preservation of KCs tolerant functions may
673 further contribute to lower inflammatory responses during YAC-MHV3 infection.
674 Altogether, results from YAC-MHV3 and 51.6-MHV3 infections strenghten the importance
675 of LSECs structural and functional integrity in restricting hepatic inflammatory response and
676 subsequent damage. In agreement, activation of LSECs towards a pro-inflammatory profile
677 was pointed out as a critical component of intrahepatic inflammation in hepatic fibrosis (40).

678

679 Differences in LSECs cytokine profile according to infection by pathogenic or attenuated
680 MHV3 strains may reflect differential PRRs induction and activation by viral fixation and/or
681 replication. We have already demonstrated that IL-6 and TNF-α production by MHV3-
682 infected macrophages resulted from TLR2 activation by the surface (S) viral protein (41).
683 The production of TNF-α by LSECs is known to depend on TLR1 to 4, -6 and -8 while IL-6
684 is produced following activation of TLR1 to 4 only (4, 17). It has been recently
685 demonstrated that TLR1/2 ligand (PamC3), but not TLR3 ligand (poly I:C) or LPS, reverted

686 the suppressive properties of LSECs (9). We have shown that virulent MHV3 strain highly
687 induced TLR2 expression on cultured LSECs and that TLR2 knockdown abrogated IL-6 and
688 CXCL1 induction only in LSECs infected by MHV3. Indeed, the proinflammatory activity
689 of MHV3 may be related to its unique abilty to induce TLR2 signalling. In agreement, lower
690 levels of inflammatory cytokines and chemokines were observed in the liver of MHV3-
691 infected TLR2 KO mice, correlating with milder hepatic damages and delayed mortality of
692 mice. Thus, TLR2 activation may represent one determining and differential factor involved
693 in the severity of virulent vs attenuated MHV3-induced hepatitis. In line with this
694 hypothesis, survival rate, inflammatory response and liver damage were similar in TLR2 KO
695 and WT mice infected by 51.6-MHV3 and were comparable to that observed in MHV3-
696 infected TLR2 KO mice. Furthermore, IL-10 levels were significantly higher in MHV3-
697 infected TLR2 KO mice, with increased expression on ECs and also on some CAV-1
698 negative cells, suggesting that specific activation of TLR2 by the virus could be one
699 mechanism by which MHV3 reverts the anti-inflammatory phenotype, at least, in LSECs.
700 Supporting this assumption, IL-10 expression was significantly up-regulated in *in vitro*
701 MHV3-infected LSECs treated with siTLR2, suggesting an inhibitory role for TLR2 on IL-
702 10 induction by MHV3. Accordingly, TLR2 activation has already been shown to
703 temporarily reverse Tregs suppressive functions (46, 47). Further work will be done to
704 identify the other IL-10-producing CAV-1-negative cells during the MHV3 infection.
705
706 TLR2 may also potentiate MHV3 infection as viral replication was significantly reduced in
707 the liver of TLR2 KO mice and in cultured LSECs rendered defective for TLR2. In addition,

activation of TLR2 by MHV3 may additionally account for its higher replication rate in LSECs since the replication of 51.6-MHV3 was not influenced by TLR2 in infected LSECs or mice. It has been demonstrated that MHV replication depends on the activation of the P38 MAPK at the beginning of the replicative cycle (48). Thus, it is conceivable that activation of TLR2 by MHV3 on LSECs optimizes P38 MAPK activation, predisposing to more efficient viral replication. Since TLR2 is also but less expressed by other resident or recruited cells in the liver, such as KCs, neutrophils and hepatocytes, as observed in preliminary experiments, we can hypothetize that several TLR2+ cells permissive to MHV3 infection may act synergistically in promoting viral replication and hepatic inflammation. Indeed, preliminary *in vitro* results revealed that production of inflammatory mediators and viral replication in MHV3-infected hepatocytes and macrophages was enhanced by TLR2. Further work is in progress to clarify the mechanistic implication of TLR2 in MHV3 replication and the role of recruited and resident TLR2+ inflammatory cells in hepatic inflammation and damage.

The differences in chemokine levels induced by the pathogenic and attenuated MHV3 strains may explain the differences in recruited intrahepatic leukocyte subsets. Indeed, lower levels of CXCL1 and CCL2 in livers from 51.6- and YAC-MHV3-infected mice correlated with delayed or lower intrahepatic recruitment of neutrophils and macrophages explaining thus the smaller inflammatory foci without extensive necrosis areas seen in livers from these mice. Unexpectedly, neutrophils were only transiently recruited and numbers of NK-T, T and B lymphocytes progressively decreased throughout MHV3 infection despite high

730 induction of chemokines. We have previously demonstrated that intrahepatic NK an NK-T
731 cells undergo higher apoptosis, and that B and T cells are stronger depleted in lymphoid
732 organs during MHV3 than YAC-MHV3 (30, 31, 49), thus altering lymphocyte recruitment
733 or turnover into the liver. The highly attenuated YAC-MHV3 infection, compared to MHV3,
734 was also related with effective activation of CD8(+) cells (32).
735
736 In addition, impairment of intrahepatic leukocyte populations and severe liver injury in
737 MHV3-infected mice may also be connected to disturbances in LSEC-derived vascular
738 factors. We have demonstrated that MHV3, unlike attenuated variants, significantly altered
739 NO release by LSECs. Susceptibility of mice to MHV3 infection has already been inversely
740 correlated with NO levels in the liver, but the mechanism was not elucidated (50). The
741 constitutive expression of NO by LSECs is essential for the regulation of intrahepatic
742 sinusoidal blood flow and protects against liver diseases. Indeed, impairment of NO release
743 by LSECs has been associated with hepatic microvascular dysfunction and portal
744 hypertension in liver pathological conditions such as fibrosis and cirrhosis (37). In cirrhotic
745 livers, NO defect has been linked to an overexpression of CAV-1 on LSECs, a negative
746 regulator of the endothelial NO synthase activity (38). We have observed that reduced NO
747 levels in LSECs correlated with a concomittent up-regulation of CAV-1, supporting that
748 MHV3-induced NO impairment is indirectly related to CAV-1 induction. Furthermore, we
749 have demonstrated that expression of the procoagulant Fgl2 increased only in LSECs
750 infected by MHV3. MHV3-induced expression of Fgl2 has already been reported in
751 endothelium of intrahepatic veins and sinusoids and was associated with severe intravascular

752 coagulation, ischemia and liver necrosis in MHV3-infected mice (28). In agreement, liver
753 histopathological analysis revelead vascular thrombosis and fibrin deposition in hepatic
754 veins and sinusoids from 48h p.i. in MHV3-infected mice only (results not shown). No
755 difference in Fgl2 levels was observed between MHV3-infected WT and TLR2 KO mice,
756 indicating that induction of Fgl2 in LSECs is TLR2-independent. Since Fgl2 expression in
757 LSECs was reported to be promoted by the MHV nucleocapsid protein and TNF-α (51, 52),
758 we can assume that higher induction of Fgl2 in the liver of MHV3-infected mice may reflect
759 higher hepatic TNF-α levels and viral replication rate in LSECs. Thus, the combined effect
760 of CAV-1/NO imbalance and Fgl2 induction during MHV3 infection may contribute to alter
761 leukocyte recruitment and aggravate hepatitis in disturbing hepatic microcirculation.
762
763 The alarmin IL-33 was shown to be up-regulated in LSECs during chronic HBV and HCV
764 infections and acute liver failure but the mechanism is elusive (21, 22). In agreement with
765 our previous report, MHV3 infection increased IL-33 production in both LSECs and
766 hepatocytes (29). Our results showed that IL-33 expression in LSECs was only increased by
767 virulent MHV3 and was not modulated by TLR2, suggesting that IL-33 release is rather a
768 consequence of MHV3-induced cell damages as necrotic cells in the liver were shown to
769 secrete alarmins such as HMGB-1 and IL-33 (53). In addition, high IL-33 serum level was
770 associated with liver damages in HBV and HCV infections, indicating that IL-33 could be
771 considered as a predictive indicator of viral hepatitis evolution, as previouly suggested (54,
772 55).
773

Using the MHV3 animal model of viral acute hepatitis, this work suggestss a novel viral-promoted mechanism of hepatic inflammation and damages involving disorders in LSEC-derived inflammatory and vascular factors. The use of MHV3 variants expressing weak tropism for LSECs allowed us to better discriminate the importance of LSECs, over other hepatic cells, in tolerance/inflammation imbalance during acute viral infection. Our results support that induction of TLR2-dependent reversion of LSECs anti-inflammatory functions by MHV3 may participate in the pathological inflammatory response that predisposes to fulminant hepatitis. Unlike MHV3, HCV and HBV do not productively infect LSECs but RNA from HCV was recently shown to induce the expression of inflammatory cytokines and chemokines in human microvascular endothelial cells via TLR3 activation (56), indicating that LSECs can be activated through PRR engagement by HCV-derived products. The "core" protein of HCV and HBV was reported to bind to TLR2 and induce TLR2-dependent inflammatory cytokine response in monocytes and macrophages (57, 58). Thus, one could presume that core proteins could also promote proinflammatory activation of LSECs via TLR2, aggravating hepatic inflammation. In this regard, a high correlation between TLR2 expression and hepatic inflammation and necrosis was demonstrated in the liver of HCV-infected patients (59).

FUNDING INFORMATION

This work was granted by NSERC of Government of Canada (grant 2895-2009 to Lucie Lamontagne) and Christian Bleau was supported by a NSERC fellowship. The funders have

795 no implication in study design, data collection and interpretation, or the decision to submit
796 the work for publication

797

798 **ACKNOWLEDGMENTS**

799 The authors want to acknowledge Corentine Lux, Pascale Bellaud and Eric Massicotte for
800 their technical assistance.

801

802

803

804

805

806

807

808

809

810

REFERENCES

1. **Tiegs G, Lohse AW**. 2010. Immune tolerance: what is unique about the liver. J Autoimmun. **34**:1-6.

2. **Xu X, Jin R, Li M, Wang K, Zhang S, Hao J, Sun X, Zhang Y, Wu H, Zhang J, Ge Q.** 2016. Liver sinusoidal endothelial cells induce tolerance of autoreactive CD4(+) recent thymic emigrants. Sci Rep. **6**:19861

3. **Thomson AW, Knolle PA**. 2010. Antigen-presenting cell function in the tolerogenic liver environment. Nat Rev Immunol **10**:753-766.

4. **Oda M, Yokomori H, Han JY**. 2003. Regulatory mechanisms of hepatic microcirculation. Clin Hemorheol Microcirc **29**:167-82.

5. **Kern M, Popov A, Scholz K, Schumak B, Djandji D, Limmer A, Eggle D, Sacher T, Zawatzky R, Holtappels R, Reddehase MJ, Hartmann G, Debey-Pascher S, Diehl L, Kalinke U, Koszinowski U, Schultze J, Knolle PA.** 2010. Virally infected mouse liver endothelial cells trigger CD8+ T-cell immunity. Gastroenterology **138**:336-346.

6. **Wu J, Meng Z, Jiang M, Zhang E, Trippler M, Broering R, Bucchi A, Krux F, Dittmer U, Yang D, Roggendorf M, Gerken G, Lu M, Schlaak JF**. 2010. Toll-like receptor-induced innate immune responses in non-parenchymal liver cells are cell type-specific. Immunology **129**:363-374.

7. **Bissel DM, Wang SS, Jarnagin WR, Roll FJ**. 1995. Cell-specific expression of transforming growth factor-beta in rat liver. Evidence for autocrine regulation of hepatocyte proliferation. J Clin Invest **96**:447–455.

833 8. **Knolle PA, Uhrig A, Hegenbarth S Löser E, Schmitt E, Gerken G, Lohse AW.** 1998.
834 IL-10 down-regulates T cell activation by antigen-presenting liver sinusoidal endothelial
835 cells through decreased antigen uptake via the mannose receptor and lowered surface
836 expression of accessory molecules. Clin Exp Immunol **114**:427–433.
837 9. **Liu J, Jiang M, Ma Z, Dietze KK, Zelinskyy G, Yang D, Dittmer U, Schlaak**
838 **JF, R oggendorf M, Lu M.** 2013. TLR1/2 ligand-stimulated mouse liver endothelial cells
839 secrete IL-12 and trigger CD8+ T cell immunity in vitro. J Immunol **191**:6178-6190.
840 10. **Lavanchy D**. 2009. The global burden of hepatitis C. Liver Int. **29**:74-81.
841 11. **Yang Q, Shi Y, Yang Y, Lou G, Chen Z**. 2015. The sterile inflammation in
842 the exacerbation of HBV-associated liver injury. Mediators Inflamm **2015**:508681.
843 12. **Bortolami M, Kotsafti A, Cardin R, Farinati F**. 2008. Fas / FasL system, IL-1beta
844 expression and apoptosis in chronic HBV and HCV liver disease. J Viral Hepat **15**:515-522.
845 13. **Barnaba V**. 2010. Hepatitis C virus infection: A "liaison a trois" amongst the virus, the
846 host, and chronic low-level inflammation for human survival. J Hepatol **53**:752–761.
847 14**. Liu M, Chan WY, McGilvray I, Ning Q, Levy GA.** 2001. Fulminant viral hepatitis:
848 molecular and cellular basis, and clinical implications. Exp Rev Mol Med **3**:1–19.
849 15. **Breiner KM, Schaller H, Knolle PA**. 2001. Endothelial cell-mediated uptake of a
850 hepatitis B virus: a new concept of liver targeting of hepatotropic microorganisms.
851 Hepatology **34**:803–808.
852 16. **Pöhlmann S, Zhang J, Baribaud F, Chen K, Leslie GJ, Lin G, Granelli- Piperno A,**
853 **Doms RW, Rice CM, McKeating JA**. 2003. Hepatitis C virus glycoproteins interact with
854 DC-SIGN and DC-SIGNR. J Virol **77**:4070–4080.

17. **Broering R, Wu J, Meng Z, Hilgard P, Lu M, Trippler M, Szczeponek A, Gerken G, Schlaak JF.** 2008. Toll-like receptor-stimulated non-parenchymal liver cells can regulate hepatitis C virus replication. J Hepatol **48**:914-922.

18. **Ludwig IS, Lekkerkerker AN, Depla E, Bosman F, Musters RJ, Depraetere S, van Kooyk Y, Geijtenbeek TB**. 2004. Hepatitis C virus targets DC SIGN and LSIGN to escape lysosomal degradation. J Virol **78**:8322-8332.

19. **Zhu CL, Yan WM, Zhu F, Zhu YF, Xi D, Tian DY, Levy G, Luo XP, Ning Q**. 2005. Fibrinogen-like protein 2 fibroleukin expression and its correlation with disease progression in murine hepatitis virus type 3-induced fulminant hepatitis and in patients with severe viral hepatitis B. World J Gastroenterol **11**:6936-6940.

20. **Foerster K, Helmy A, Zhu Y, Khattar R, Adeyi OA, Wong KM, Shalev I, Clark DA, Wong PY, Heathcote EJ, Phillips MJ, Grant DR, Renner EL, Levy GA, Selzner N.**2010.The novel immunoregulatory molecule FGL2a potential biomarker for severity chro nic hepatitis C virus infection. J Hepatol **53**:608-615.

21. **Marvie P, Lisbonne M, L'Helgoualc'h A, Rauch M, Turlin B, Preisser L, Bourd-Boittin K, Théret N, Gascan H, Piquet-Pellorce C, Samson M**. 2010. Interleukin-33 overexpression is associated with liver fibrosis in mice and humans. J Cell Mol Med **14**: 1726-1739.

22. **Roth GA, Zimmermann M, Lubsczyk BA, Pilz J, Faybik P, Hetz H, Hacker S, Mangold A, Bacher A, Krenn CG, Ankersmit HJ**. 2010. Up-regulation of interleukin 33 and soluble ST2 serum levels in liver failure. J Surg Res **163**:e79-e83.

876 23. **Le Prevost C, Virelizier JL, Dupuy JM**. 1975. Immunopathology of mouse hepatitis
877 virus type 3 infection. III. Clinical and virologic observation of a persistent viral infection. J
878 Immunol **115**:640-645.
879 24. **Martin JP, ChenW, Koehren F, Pereira CA**. 1994. The virulence of mouse hepatitis
880 virus 3, as evidenced by permissivity of cultured hepatic cells toward escaped mutants. Res
881 Virol **145**:297–302.
882 25. **Belouzard S, Millet JK, Licitra BN, Whittaker GR**. 2012. Mechanisms of coronavirus
883 cell entry mediated by the viral spike protein. Viruses **4**:1011-1033.
884 26. **Pereira CA, Steffan AM, Kirn A**. 1984. Interaction between mouse hepatitis viruses
885 and primary cultures of Kupffer and endothelial liver cells from resistant and susceptible
886 inbred mouse strains. J Gen Virol **65**:1617–20.
887 27. **Steffan AM, Pereira CA, Bingen A, V alle M, Martin JP, Koehren F, Royer**
888 **C, Gendrault JL, Kirn A**. 1995. Mouse hepatitis virus type 3 infection provokes a decrease
889 in the number of sinusoidal endothelial cell fenestrae both in vivo and in vitro.
890 Hepatology **22**:395-401.
891 28. **Marsden PA, Ning Q, Fung S, Luo X, Chen Y, Mendicino M, Ghanekar A, Scott**
892 **JA, Miller T, Chan CW, Chan MW, He W, Gorczynski RM, Grant DR, Clark DA,**
893 **Phillips MJ, Levy GA.** 2003. The Fgl2/fibroleukin prothrombinase contributes to
894 immunologically mediated thrombosis in experimental and human viral hepatitis. J Clin
895 Invest **112**:58-6626.
896 29. **Arshad MI, Patrat-Delon S, Piquet-Pellorce C, L'helgoualc'h A, Rauch M, Genet**
897 **V, Lucas-Clerc C, Bleau C, Lamontagne L, Samson M.** 2013. Pathogenic mouse hepatitis

virus or poly(I:C) induce IL-33 in hepatocytes in murine models of hepatitis. PLoS One **8**:e74278.

30. **Jacques A, Bleau C, Martin JP, Lamontagne L**. 2008. Intrahepatic endothelial and Kupffer cells involved in immunosuppressive cytokines and natural killer (NK)/NK T cell disorders in viral acute hepatitis. Clin Exp Immunol. **152**:298-310

31**. Lehoux M, Jacques A, Lusignan S, Lamontagne L**. 2004. Murine viral hepatitis involves NK cell depletion associated with virus-induced apoptosis.Clin Exp Immunol. 137:41-51.

32**. Lamontagne L, Lusignan S, Page C.** 2001. Recovery from mouse hepatitis virus infection depends on recruitment of CD8(+) cells rather than activation of intrahepatic CD4(+)alphabeta(-)TCR(inter) or NK-T cells. Clin Immunol **101**:345-356.

33. **Schrage A, Loddenkemper C, Erben U, Lauer U, Hausdorf G, Jungblut PR, Johnson J, Knolle PA, Zeitz M, Hamann A, Klugewitz K**. 2008. Murine CD146 is widely expressed on endothelial cells and is recognized by the monoclonal antibody ME-9F1. Histochem Cell Biol **129**:441-451.

34. **Yamazaki H, Oda M, Takahashi Y, Iguchi H, Yoshimura K, Okada N, Yokomori H**. 2013. Relation between ultrastructural localization, changes in caveolin-1, and capillarization of liver sinusoidal endothelial cells in human hepatitis C-related cirrhotic liver. J Histochem Cytochem **61**:169-76.

35. **Neumann K, Erben U, Kruse N, Wechsung K, Schumann M, Klugewitz K, Scheffold A, Kühl AA**. 2015. Chemokine transfer by liver sinusoidal endothelial cells contributes to the recruitment of CD4+ T cells into the murine liver. PLoS One **10**:e0123867.

921 36. **Pope M, Marsden PA, Cole E, Sloan S, Fung LS, Ning Q, Ding JW, Leibowitz JL,**
922 **Phillips MJ, Levy GA**. 1998. Resistance to murine hepatitis virus strain 3 is dependent on
923 production of nitric oxide. J Virol **72**:7084-90.
924 37. **Iwakiri Y, Kim MY**. 2015. Nitric oxide in liver diseases. Trends Pharmacol Sci **36**:
925 524-536.
926 38. **Yokomori H, Oda M, Yoshimura K, Nomura M, Wakabayashi G, Kitajima M, Ishii**
927 **H**. 2003. Elevated expression of caveolin-1 at protein and mRNA level in human cirrhotic
928 liver: Relation with nitric oxide. J Gastroenterol **38**:854–860
929 39. **Peyrefitte CN, Pastorino B, Grau GE, Lou J, Tolou H, Couissinier-Paris P**. 2006.
930 Dengue virus infection of human microvascular endothelial cells from different vascular
931 beds promotes both common and specific functional changes. J Med Virol **78**:229-42.
932 40. **Connolly MK, Bedrosian AS, Malhotra A, Henning JR, Ibrahim J, Vera V, Cieza-**
933 **Rubio NE, Hassan BU, Pachter HL, Cohen S, Frey AB, Miller G**. 2010. In hepatic
934 fibrosis, liver sinusoidal endothelial cells acquire enhanced immunogenicity. J Immunol
935 **185**:2200-2208.
936 41. **Jacques A, Bleau C, Turbide C, Beauchemin N, Lamontagne L**. 2009. Macrophage
937 interleukin-6 and tumour necrosis factor-alpha are induced by coronavirus fixation to Toll-
938 like receptor 2/heparan sulphate receptors but not carcinoembryonic cell adhesion antigen
939 1a. Immunology **128**:e181-192.

940 42. **Ganesan LP, Mohanty S, Kim J, Clark KR, Robinson JM, Anderson CL**. 2011.
941 Rapid and efficient clearance of blood-borne virus by liver sinusoidal endothelium. PLoS
942 Pathog **7:**e1002281.

943 43. **Simon-Santamaria J, Rinaldo CH, Kardas P, Li R, Malovic I, Elvevold K, McCourt**
944 **P, Smedsrød B, Hirsch HH, Sørensen KK**. 2014. Efficient uptake of blood-borne BK and
945 JC polyomavirus-like particles in endothelial cells of liver sinusoids and renal vasa recta.
946 PLoS One **9**:e111762.

947 44. **Carambia A, Frenzel C, Bruns OT, Schwinge D, Reimer R, Hohenberg H, Huber**
948 **S, Tiegs G, Schramm C, Lohse AW, Herkel J**. 2013. Inhibition of inflammatory CD4 T
949 cell activity by murine liver sinusoidal endothelial cells. J Hepatol. 2013 **58**:112-8.

950 45. **Lamontagne L, Dupuy JM**. 1987. Characterization of a non
951 pathogenic MHV3 variant derived from a persistently infected lymphoid cell line. Adv Exp
952 Med Biol. **218**:255-63

953 46. **Sutmuller RP, den Brok MH, Kramer M, Bennink EJ, Toonen LW, Kullberg BJ,**
954 **Joosten LA, Akira S, Netea MG, Adema GJ**. 2006. Toll-like receptor 2 controls
955 expansion and function of regulatory T cells. J Clin Invest **116**:485-94.

956 47. **Liu G, Zhao Y.** 2007. Toll-like receptors and immune regulation: their direct and
957 indirect modulation on regulatory CD4+ CD25 + T cells. Immunology **122**:149-56.

958 48. **Banerjee S, Narayanan K, Mizutani T, Makino S**. 2002. Murine coronavirus
959 replication-induced p38 mitogen-activated protein kinase activation promotes interleukin-6
960 production and virus replication in cultured cells. J Virol **76**:5937–48.

961 49. **Lamontagne L, Descoteaux JP, Jolicoeur P**. 1989. Mouse hepatitis virus 3 replication
962 in T and B lymphocytes correlate with viral pathogenicity. J Immunol **142**:4458–4465.
963 50. **Tsuhako MH, Augusto O, Linares E, Dagli ML, Pereira CA**. 2006. Association
964 between nitric oxide synthesis and vaccination-acquired resistance to murine hepatitis virus
965 by SPF mice. Free Radic Biol Med **41**:1534-1541
966 51. **Ning Q, Liu M, Kongkham P, Lai MM, Marsden PA, Tseng J, Pereira B,**
967 **Belyavskyi M, Leibowitz J, Phillips MJ, Levy G**. 1999. The nucleocapsid protein of
968 murine hepatitis virus type 3 induces transcription of the novel fgl2 prothrombinase gene. J
969 Biol Chem **274**:9930-9936.
970 52. **Liu J, Tan Y, Zhang J, Zou L, Deng G, Xu X, Wang F, Ma Z, Zhang J, Zhao**
971 **T, Liu Y, Li Y, Zhu B., Guo B.** 2015. C5aR, TNF-α, and FGL2 contribute to coagulation
972 and complement activation in virus-induced fulminant hepatitis. J Hepatol **62**:354–362.
973 53. **Arshad MI, Piquet-Pellorce C, Samson M.** 2012. IL-33 and HMGB1 alarmins:
974 Sensors of cellular death and their involvement in liver pathology. Liver Internat **32**:1200–
975 1210.
976 54. **Wang J, Zhao P, Guo H, Sun X, Jiang Z, Xu L, Feng J, Niu J, Jiang Y**. 2012 Serum
977 IL-33 levels are associated with liver damage in patients with chronic hepatitis C. Mediat
978 Inflam **2012**:819636.
979 55. **Wang J, Cai Y, Ji H, Feng J, Ayana DA, Niu J, Jiang Y.** 2012 Serum IL-33 levels are
980 associated with liver damage in patients with chronic hepatitis B. J Interferon Cytokine Res
981 **32**:248-253.

982 56. **Pircher J, Czermak T, Merkle M, Mannell H, Krötz F, Ribeiro A, Vielhauer V, Nadjiri**
983 **J, Gaitzsch E, Niemeyer M, Porubsky S, Gröne HJ, Wörnle M.** 2014. Hepatitis C virus
984 induced endothelial inflammatory response depends on the functional expression of TNFα
985 receptor subtype 2. PLoS One **9**:e113351.
986 57. **Cooper A, Tal G, Lider O, Shaul Y**. 2005. Cytokine induction by the hepatitis B virus
987 capsid in macrophages is facilitated by membrane heparan sulfate and involves TLR2. J
988 Immunol **175**:3165–76.
989 58. **Dolganiuc A, Oak S, Kodys K, Golenbock DT, Finberg RW, Kurt-Jones E, Szabo G**.
990 2004. Hepatitis C core and nonstructural 3 proteins trigger toll-like receptor 2-mediated
991 pathways and inflammatory activation. Gastroenterology **127**:1513–24.
992 59. **Berzsenyi MD, Roberts SK, Preiss S, Woollard DJ, Beard MR, Skinner NA, Bowden**
993 **DS, Visvanathan K**. 2011. Hepatic TLR2 & TLR4 expression correlates with hepatic
994 inflammation and TNF-α in HCV & HCV/HIV infection. J Viral Hepat **18**:852–60.
995
996
997
998
999
1000
1001
1002
1003
1004

LEGENDS OF FIGURES

Figure 1: Hepatic damages and viral replication in highly hepatotropic MHV3- and attenuated 51.6- and YAC-MHV3-infected mice. Groups of 5 or 6 C57BL/6 were intraperitoneally infected with 1000 $TCID_{50}$ (tissue culture infective dose 50%) of MHV3, 51.6-MHV3 or YAC-MHV3. (A) Histopathological analysis was conducted on livers from mock- and viral-infected mice from each group at 24 and 72 h p.i. Inflammatory and necrosis foci are indicated by arrows. (B) Summary of occurrence of necrotic and inflammatory foci in livers from infected mice at 24, 48 and 72 h p.i. ALT (C) and AST (D) activities were assayed in serum samples from mock- and viral-infected mice at 24, 48 and 72 h p.i. MHV3 replication in livers from each group of infected mice was determined by analysis of the nucleoprotein (NP) RNA expression at 24, 48 and 72 h p.i. by RT-qPCR (E) and by viral titration ($TCID_{50}$) (D) at 24 h and 72 h p.i. Values represent fold change in gene expression relative to mock-infected mice after normalisation with HPRT expression. Arrows indicate inflammatory or necrosis foci. Values are means plus standard errors of the mean (error bars). ***$P < 0{\cdot}001$ when compared with mock-infected mice and ††$P < 0{\cdot}01$; †††$P < 0{\cdot}001$ when compared with MHV3-infected group.

Figure 2: Gene expression and/or production of Caveolin-1, Fgl2 and IL-33 in the liver of MHV3-, 51.6-MHV3- and YAC-MHV3-infected mice. Groups of 5 or 6 C57BL/6 (WT) were intraperitoneally infected with 1000 $TCID_{50}$ (tissue culture infective dose 50%)

of MHV3, 51.6-MHV3 and YAC-MHV3. At 24, 48 or 72 h p.i., livers were collected from mock- and viral-infected mice of each group. mRNA expression for (A) caveolin -1, (C) Fgl-2, and (D) IL-33 genes was evaluated by qRT-PCR. Values represent fold change in gene expression relative to mock-infected mice (arbitrarily taken as 1) after normalisation with HPRT expression. *In situ* expression of caveolin-1 (B) and IL-33 (F) were determined by immunohistochemistry in livers from mock-, MHV3- and 51.6-MHV3-infected mice at 48 h p.i. Caveolin-1 and IL-33 positive cells are indicated by arrows. Production levels of IL-33 (E) were quantified by ELISA at 72 h p.i. in the liver of each mouse. Immunolocalization of IL-33 in LSECs (G) was confirmed by double immunostaining of IL-33 (green) and CAV-1 (red) in livers from mock- and MHV3-infected mice at 48 and 72 h p.i. Cell nuclei were counterstained with Hoescht (blue). *In situ* expressions of caveolin-1 (B) or IL-10 and caveolin-1 (G) by endothelial cell are indicated by arrows. Values are means plus standard errors of the mean (error bars). *$P < 0{\cdot}05$; **$P < 0{\cdot}01$; ***$P < 0{\cdot}001$ when compared with mock-infected mice, and †$P < 0{\cdot}05$; ††$P < 0{\cdot}01$; †††$P < 0{\cdot}001$ when compared with MHV3-infected group.

Figure 3: Gene expression and production of IL-10, TGF-β, IL-6, TNF-α, CXCL1, CCL2 and CXCL10 in the liver of MHV3-, 51.6-MHV3- and YAC-MHV3-infected mice. Groups of 5 or 6 C57BL/6 mice were intraperitoneally infected with 1000 $TCID_{50}$ (tissue culture infective dose 50%) of MHV3, 51.6-MHV3 and YAC-MHV3. At 24, 48 or 72 h p.i., livers were collected from mock- and viral-infected mice of each group. **Section I:** (A) IL-10, (C) TGF-β, (E) IL-6, and (G) TNF-α mRNA fold changes were analyzed by

qRT-PCR. Values represent fold change in gene expression relative to mock-infected mice (arbitrarily taken as 1) after normalisation with HPRT expression. Production levels of (B) IL-10, (D) TGF-β, (F) IL-6, and (H) TNF-α were quantified by ELISA test at 72 h p.i. in the liver of each mouse. **Section II**: *In situ* expression of IL-10 and caveolin-1 was assayed by immunohistochemistry in livers of mock-, MHV3- and 51.6-MHV3-infected mice at 48 h p.i. (arrows show IL-10 and Caveolin-1-expressing endothelial cells) **Section III**: (A) CXCL1, (C) CCL2, and (E) CXCL10 mRNA fold changes were analyzed by qRT-PCR. Values represent fold change in gene expression relative to mock-infected mice (arbitrarily taken as 1) after normalisation with HPRT expression. Production levels of (B) CXCL1, (D) CCL2, and (F) CXCL10 were quantified by ELISA at 72 h p.i. in the liver of each mouse Values are means plus standard errors of the mean (error bars). *$P < 0{\cdot}05$; **$P < 0{\cdot}01$; ***$P < 0{\cdot}001$ when compared with mock-infected mice, and †$P < 0{\cdot}05$; ††$P < 0{\cdot}01$; †††$P < 0{\cdot}001$ when compared with MHV3-infected group.

Figure 4: Gene expression of TLR2, 3, 4, 7 and helicases RIG-I and MDA5 in the liver of MHV3-, 51.6-MHV3- and YAC-MHV3-infected mice. Groups of 5 or 6 C57BL/6 (WT) were intraperitoneally infected with 1000 $TCID_{50}$ (tissue culture infective dose 50%) of MHV3, 51.6-MHV3 and YAC-MHV3. At 24, 48 or 72 h p.i., livers were collected from mock- and viral-infected mice of each group. mRNA expression for (A) TLR2, (B) TLR3, (C) TLR4, (D) TLR7, (E) RIG-I and (F) MDA5 genes was evaluated by qRT-PCR. Values represent fold change in gene expression relative to mock-infected mice (arbitrarily taken as 1) after normalisation with HPRT expression. Values are means plus standard errors of the

mean (error bars). *$P < 0{\cdot}05$; **$P < 0{\cdot}01$; ***$P < 0{\cdot}001$ when compared with mock-infected mice, and †$P < 0{\cdot}05$; ††$P < 0{\cdot}01$; †††$P < 0{\cdot}001$ when compared with MHV3-infected group.

Figure 5: Percentages and numbers of intrahepatic mononuclear cell subsets in livers from MHV3-, 51.6-MHV3 and YAC-MHV3-infected mice. Intrahepatic mononuclear cells were isolated from groups of 5 or 6 mock-infected or MHV3-, 51.6-MHV3 and YAC-MHV3-infected C57BL/6 mice at 24 and 48 h p.i., immunolabeled with NK1.1, CD3, Gr1, CD11b, CD19, CD4 and CD8 monoclonal antibodies and analyzed by cytofluorometry. Percentages of (A) NKT (NK1.1+CD3+), (B) NK (NK1.1+CD3), (C) neutrophils ($Gr1^{hi}$ $CD11b^{hi}$), (D) macrophages ($Gr1^{+}$ $CD11b^{int}$) cells, (E) (CD19+), (F) CD4 (CD3+CD4+) and (G) CD8 (CD3+CD8+) were evaluated in livers from each group of infected mice (section I). Absolute numbers for each cell subset (calculated in using respective percentages reported to total number of isolated mononuclear cells) were similarly recorded in livers of respective groups (section II). Values are means plus standard errors of the mean (error bars). *$P < 0{\cdot}05$; **$P < 0{\cdot}01$; ***$P < 0{\cdot}001$ when compared with mock-infected mice, and †$P < 0{\cdot}05$; ††$P < 0{\cdot}01$; †††$P < 0{\cdot}001$ when compared with MHV3-infected group.

Figure 6: Permissivity of LSECs to MHV3, 51.6-MHV3 and YAC-MHV3 infection. Mouse LSECs were isolated by Percoll gradient and enriched by immunomagnetism with anti-CD146 antibodies. (A) LSECs were characterized by immunolabelling with antibodies for CD146, CD54, CD31 and F4/80 cell markers and cyrofluorometric analysis. B-C)

LSECs were infected at 0.1 MOI of MHV3, 51.6-MHV3 and YAC-MHV3 and the evolution of cytopathic effects was noted in LSEC cultures up to 5 days p.i. (B). The kinetics of MHV infections were monitored by quantifying viral titers in supernatants of infected LSECs (C). All experiments were conducted in triplicate. Results are representative of two independent experiments.Values are means for each point. †††$P < 0{\cdot}001$ when compared with MHV3-infected cells.

Figure 7: Expression levels of Fgl2, IL-33 and caveolin-1, and production of NO in *in vitro* MHV3-, 51.6-MHV3 and YAC-MHV3-infected LSECs. LSECs were infected at 0.1 MOI of MHV3, 51.6-MHV3 and YAC-MHV3 and RNA and supernantant from LSECs infected with each viral strain were collected at 24, 48 or 72 h p.i. (A) IL-33, (C) Fgl-2, and (E) caveolin-1 mRNA fold changes were analyzed by qRT-PCR. Values represent fold change in gene expression relative to uninfected LSECs (control arbitrarily taken as 1) after normalisation with HPRT expression. All samples were run in duplicate. (B) Production levels of IL-33 were quantified by ELISA and NO levels (D) were assayed by the Griess reaction in supernatants at 48 h p.i. All experiments were run in duplicate and results are representative of two independent experiments. Values are means plus standard errors of the mean (error bars). *$P < 0{\cdot}05$; **$P < 0{\cdot}01$; ***$P < 0{\cdot}001$ when compared with mock-infected cells, and †$P < 0{\cdot}05$; ††$P < 0{\cdot}01$; †††$P < 0{\cdot}001$ when compared with MHV3-infected cells.

Figure 8: Gene expression and production of IL-10, TGF-β, IL-6, TNF-α, CXCL1, CCL2 and CXCL10 in *in vitro* MHV3-, 51.6-MHV3- and YAC-MHV3-infected LSECs. LSECs were infected at 0.1 MOI of MHV3, 51.6-MHV3 and YAC-MHV3 and RNA and supernantant from LSECs infected with each viral strain were collected at 24, 48 or 72 h p.i. **Section I:** (A) IL-10, (C) TGF-β, (E) IL-6, and (G) TNF-α mRNA fold changes were analyzed by qRT-PCR. Values represent fold change in gene expression relative to uninfected LSECs (control arbitrarily taken as 1) after normalisation with HPRT expression. All samples were run in duplicate. Production levels of (B) IL-10, (D) TGF-β, (F) IL-6, and (H) TNF-α were quantified by ELISA in supernatants at 24 h p.i. **Section II**: (A) CXCL1, (C) CCL2, and (E) CXCL10 mRNA fold changes were analyzed by qRT-PCR. Values represent fold change in gene expression relative to control (uninfected) LSECs after normalisation with HPRT expression. All samples were run in duplicate. Production levels of (B) CXCL1, (D) CCL2, and (F) CXCL10 were quantified by ELISA in supernatants at 24 h p.i. All experiments were conducted in duplicate and results are representative of two independent experiments. Values are means plus standard errors of the mean (error bars). $*P < 0{\cdot}05$; $**P < 0{\cdot}01$; $***P < 0{\cdot}001$ when compared with mock-infected cells, and †$P <$ 0·05; ††$P < 0{\cdot}01$; †††$P < 0{\cdot}001$ when compared with MHV3-infected cells.

Figure 9: Role of TLR2 in viral replication and expression of IL-6 and CXCL1 in MHV3- 51.6-MHV3- and YAC-MHV3-infected LSECs. A) LSECs were infected at 0.1 MOI of MHV3, 51.6-MHV3 and YAC-MHV3. At 24, 48 and 72 h p.i., RNA from infected LSECs was extracted and mRNA expression levels for TLR2 gene was determined by qRT-

PCR. B to D) LSECs were treated with specific siRNA against TLR2 prior to infection with viruses or treatment with the specific TLR2 agonist Pam3Cys (as positive control) for 24h. (B) MHV nucleoprotein (MHV-N), (C) IL-6, and (D) CXCL1 mRNA expression levels were determined by qRT-PCR. Values represent fold change in gene expression relative to control (uninfected) LSECs after normalisation with HPRT expression. All samples were run in duplicate and results are representative of two independent experiments. *$P < 0{\cdot}05$; **$P < 0{\cdot}01$; ***$P < 0{\cdot}001$ when compared with ctrl cells, and †$P < 0{\cdot}05$ when compared with MHV3-infected cells.

Figure 10: Mortality, hepatic damages and viral replication in MHV3- and 51.6-MHV3-infected C57BL/6 (WT) and TLR2 KO mice. Groups of 6 or 7 C57BL/6 (WT) and TLR2 KO mice were intraperitoneally (i.p.) infected with 1000 $TCID_{50}$ (tissue culture infective dose 50%) of MHV3 and 51.6-MHV3. Percentages of (A) MHV3- and (B) 51.6-MHV3-infected surviving mice were recorded at various times post-infection (p.i.). (C) Histopathological analysis was conducted on livers from mock-, MHV3- and 51.6-MHV3-infected WT and TLR2 KO at 72 h p.i. Necrosis foci are indicated by arrows (D) MHV3 and 51.6-MHV3 replication in livers from infected WT and TLR2 KO mice was determined by viral titration ($TCID_{50}$) at 24 h and 72 h p.i. Values are means plus standard errors of the mean (error bars). Results are representative of two different experiments. ***$P < 0{\cdot}001$ when compared with WT mice.

Figure 11: Expression of IL-10 and Caveolin-1 in livers from MHV3-infected TLR2 KO mice. Groups of 6 TLR2 KO mice were intraperitoneally (i.p.) infected with 1000 $TCID_{50}$ (tissue culture infective dose 50%) of MHV3 and immunolocalization of IL-10 in the liver and ECs of mock- and MHV3-infected TLR2 KO mice was determined by double immunostaining of IL-10 (green) and Caveolin-1 (CAV) (red) at 48 h p.i. Cell nuclei were counterstained with Hoescht (blue). *In situ* expressions of IL-10 and caveolin-1 by endothelial cell are indicated by arrows.

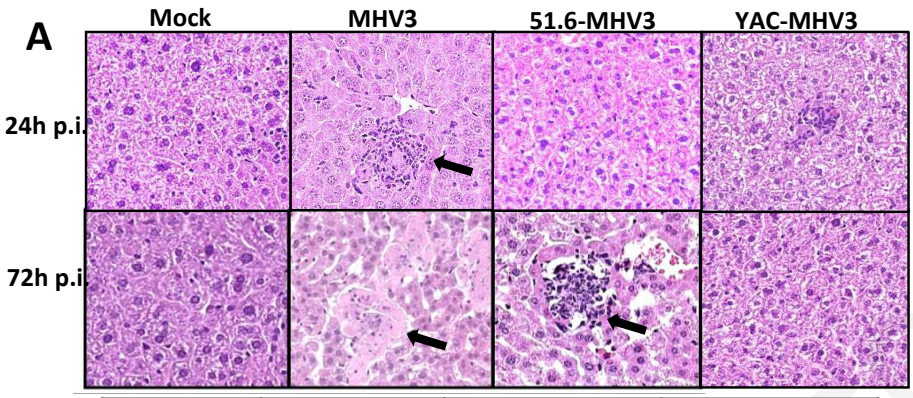

B

Virus	Time p.i. (hrs)	Inflammatory foci	Hepatic necrosis foci
MHV3	24	++	-
	48	++	++
	72	+	++++
51.6-MHV3	24	-	-
	48	+	+
	72	++	+
YAC-MHV3	24	+	-
	48	+	-
	72	+	-

+ (scarse foci); ++ (10% of hepatic tissue); +++ (20-30% of hepatic tissue);
++++ (up to 40% of hepatic tissue)

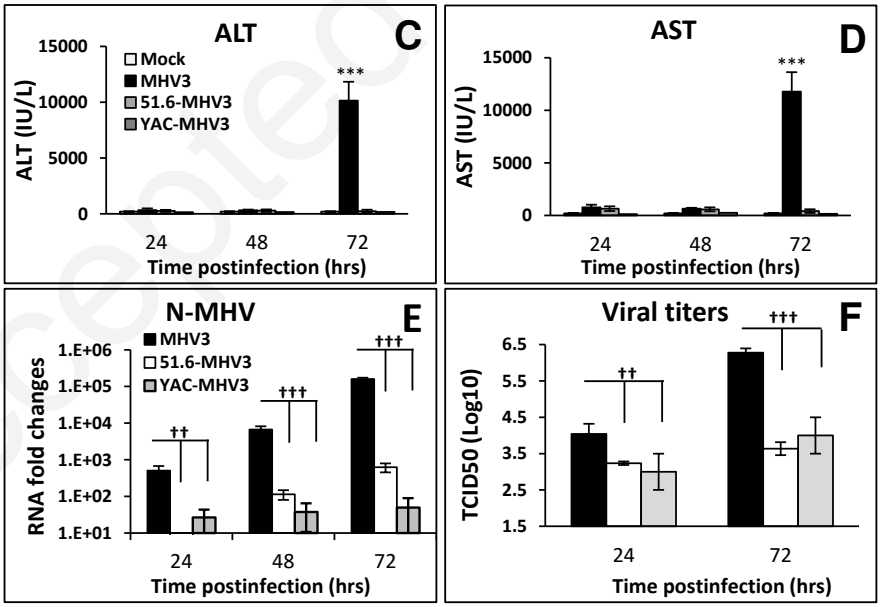

Figure 1

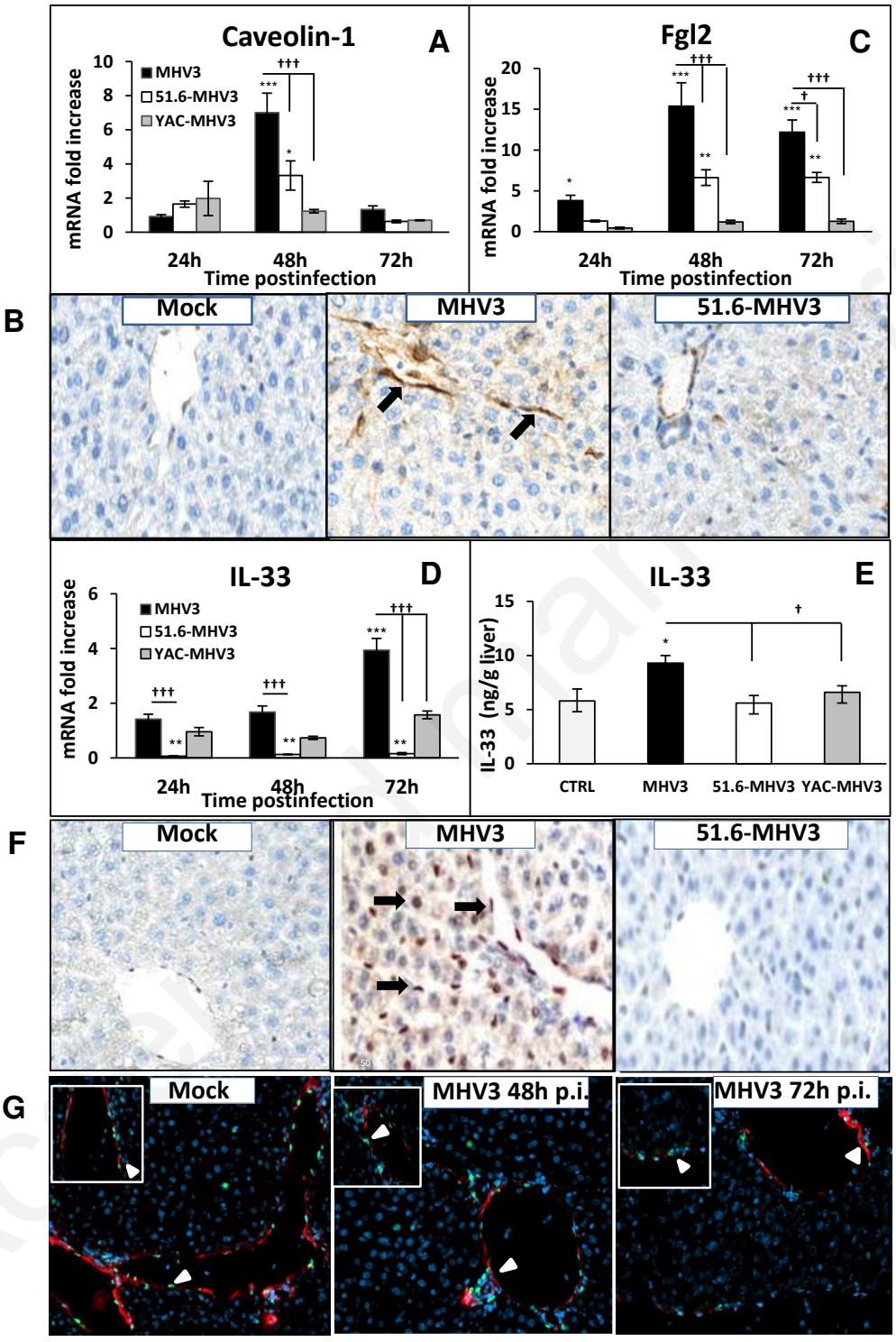
Caveolin-1
A
mRNA fold increase
MHV3
51.6-MHV3
YAC-MHV3
24h
48h
72h
Time postinfection
Fgl2
C
B
Mock
MHV3
51.6-MHV3
IL-33
D
E
IL-33 (ng/g liver)
CTRL
F
G
MHV3 48h p.i.
MHV3 72h p.i.

Figure 2

I)

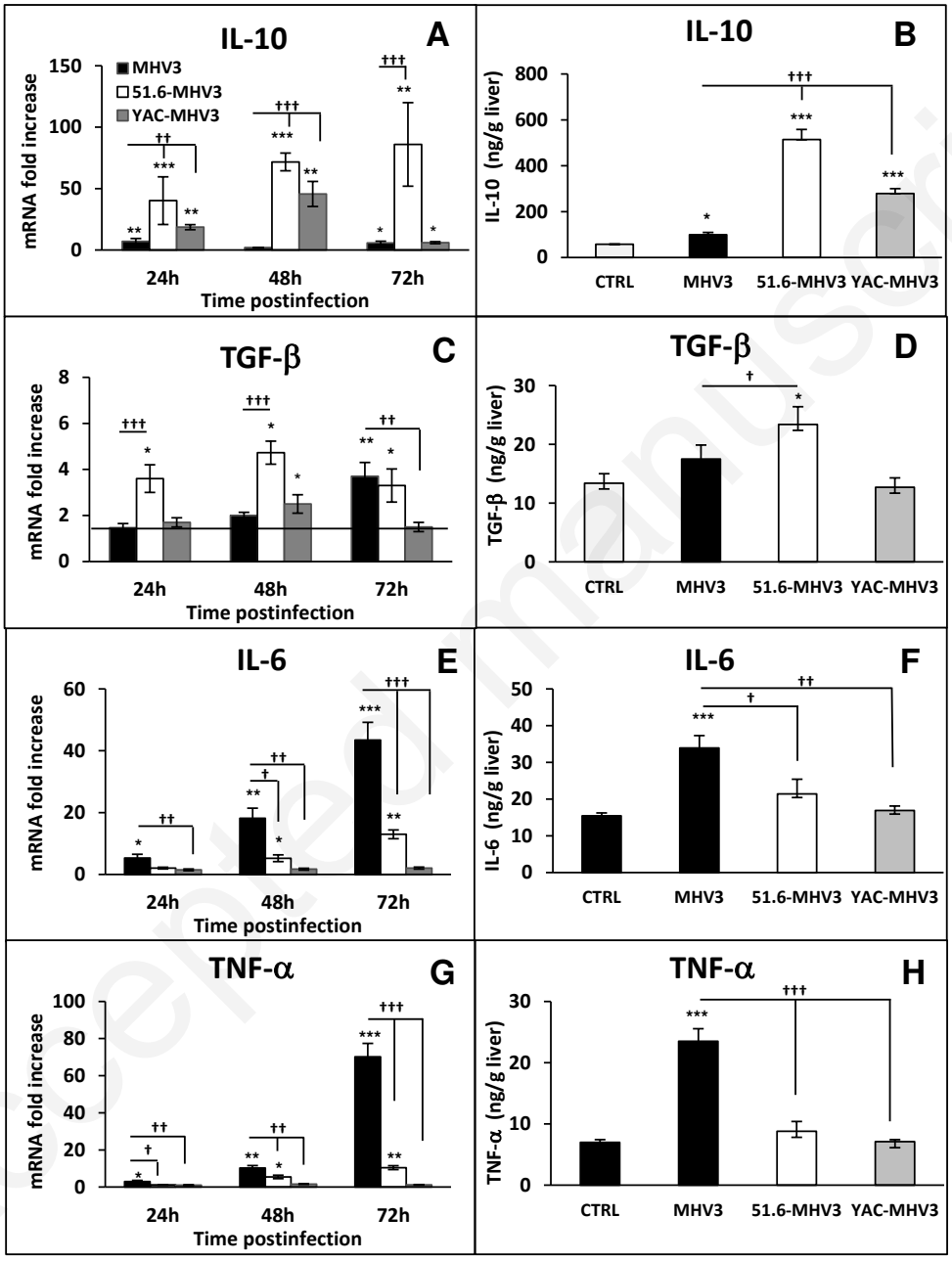

Figure 3
(section I)

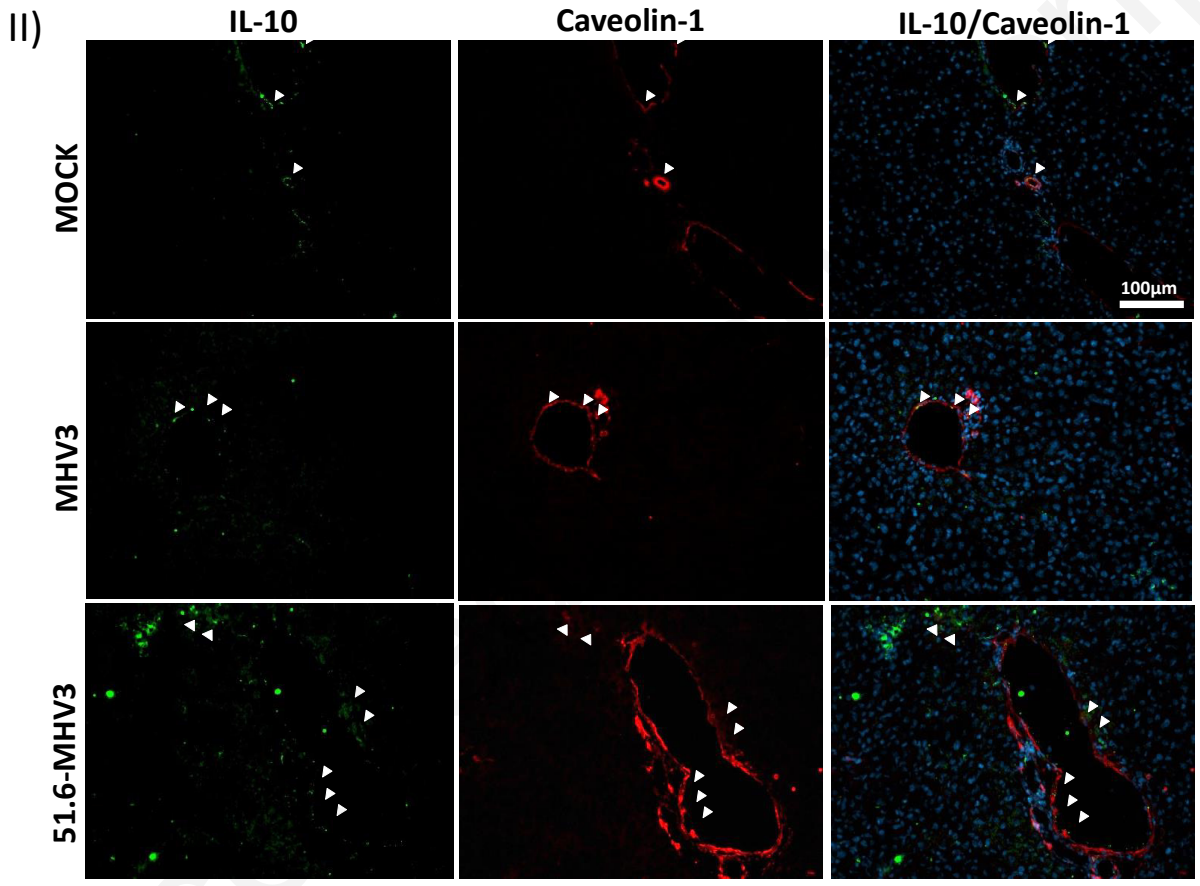

Figure 3
(Section II)

III)

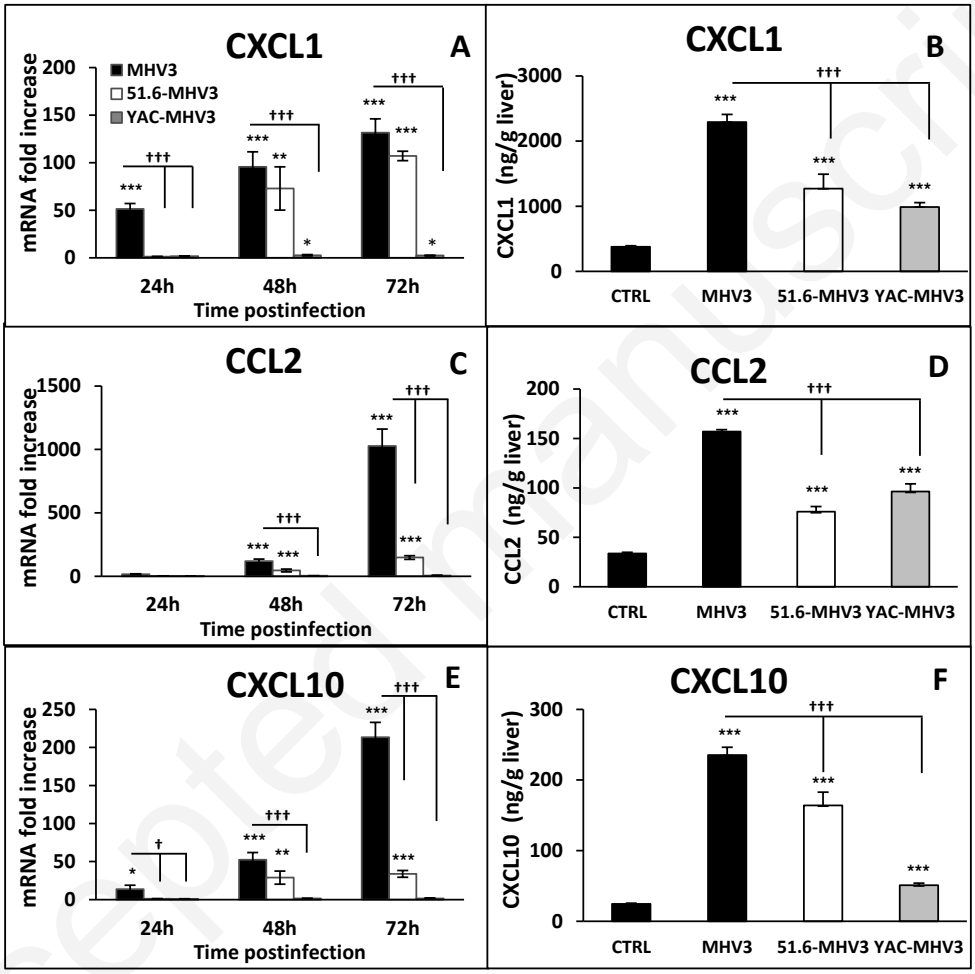

Figure 3
(section III)

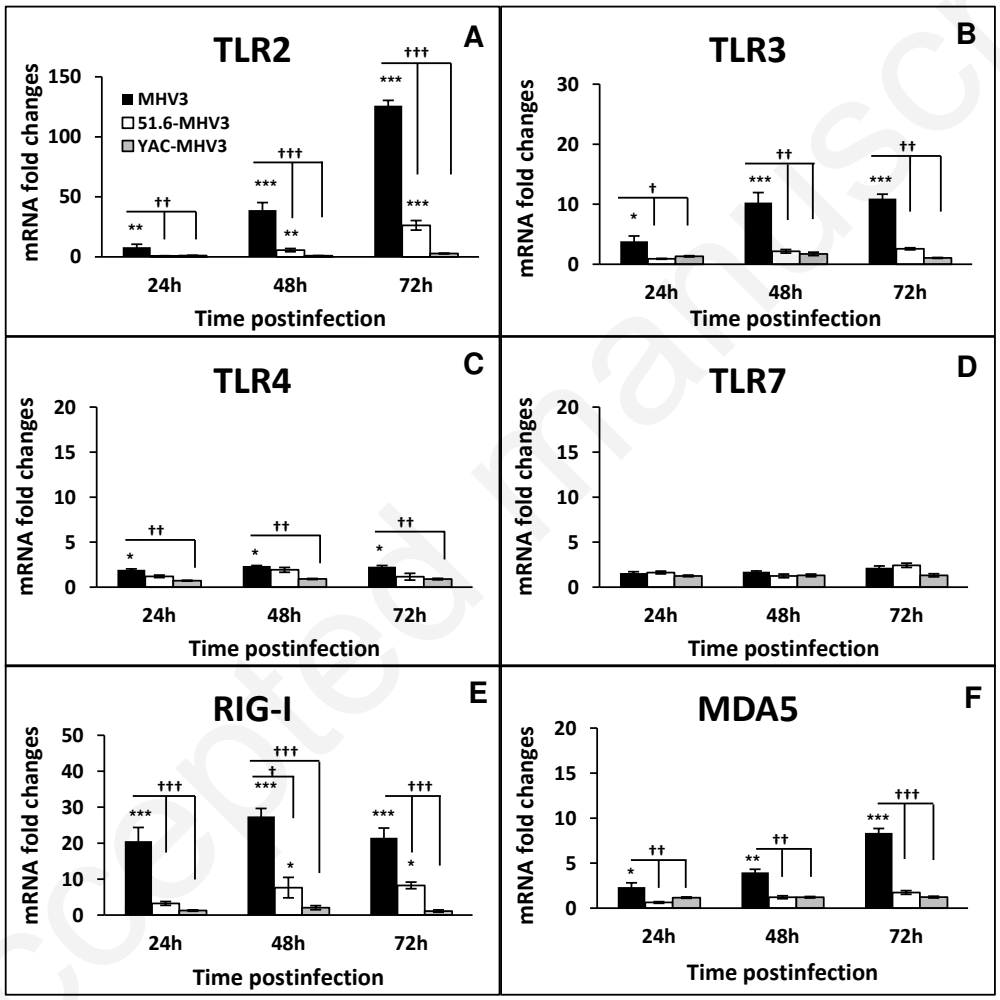

Figure 4

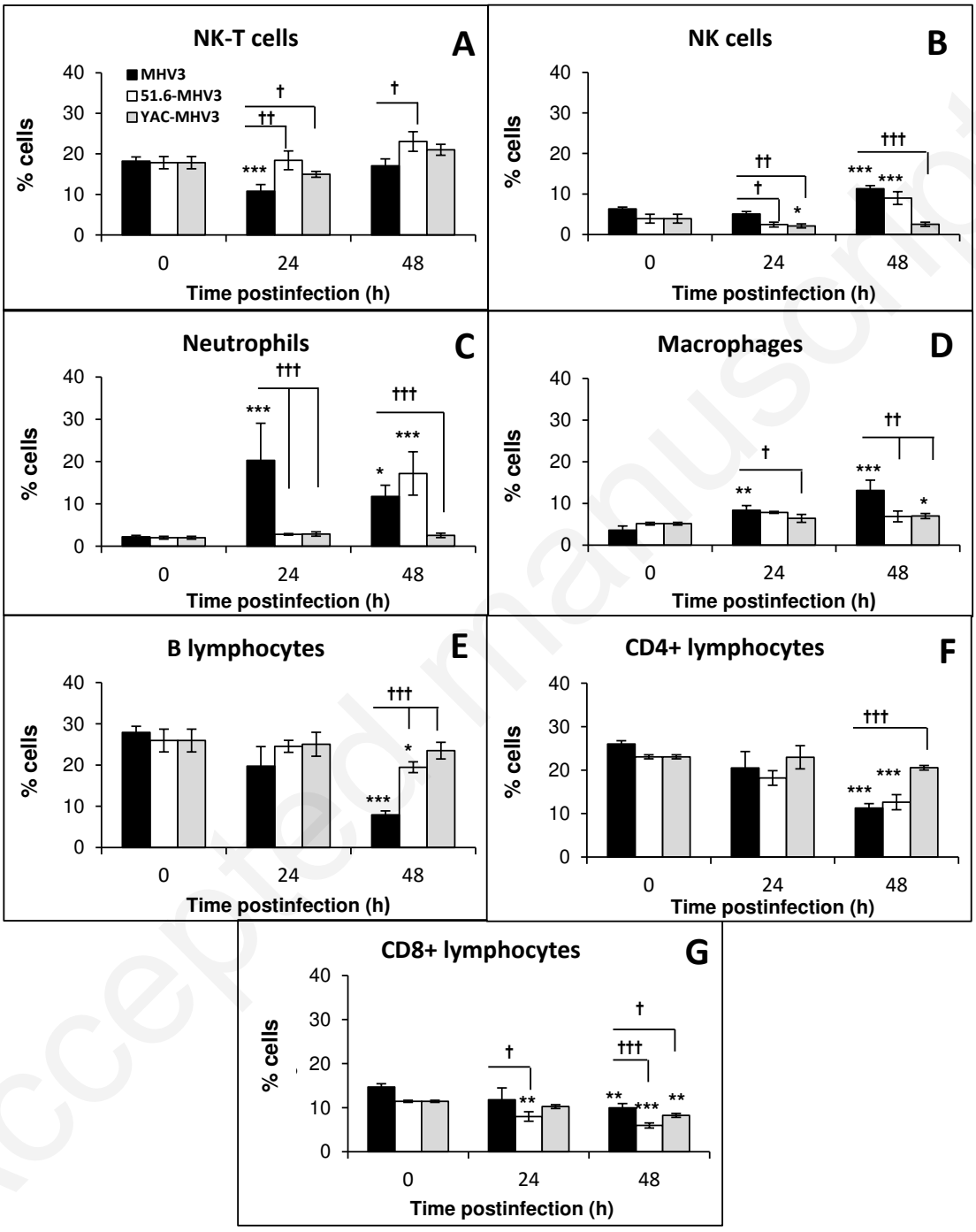

Figure 5
(Section I)

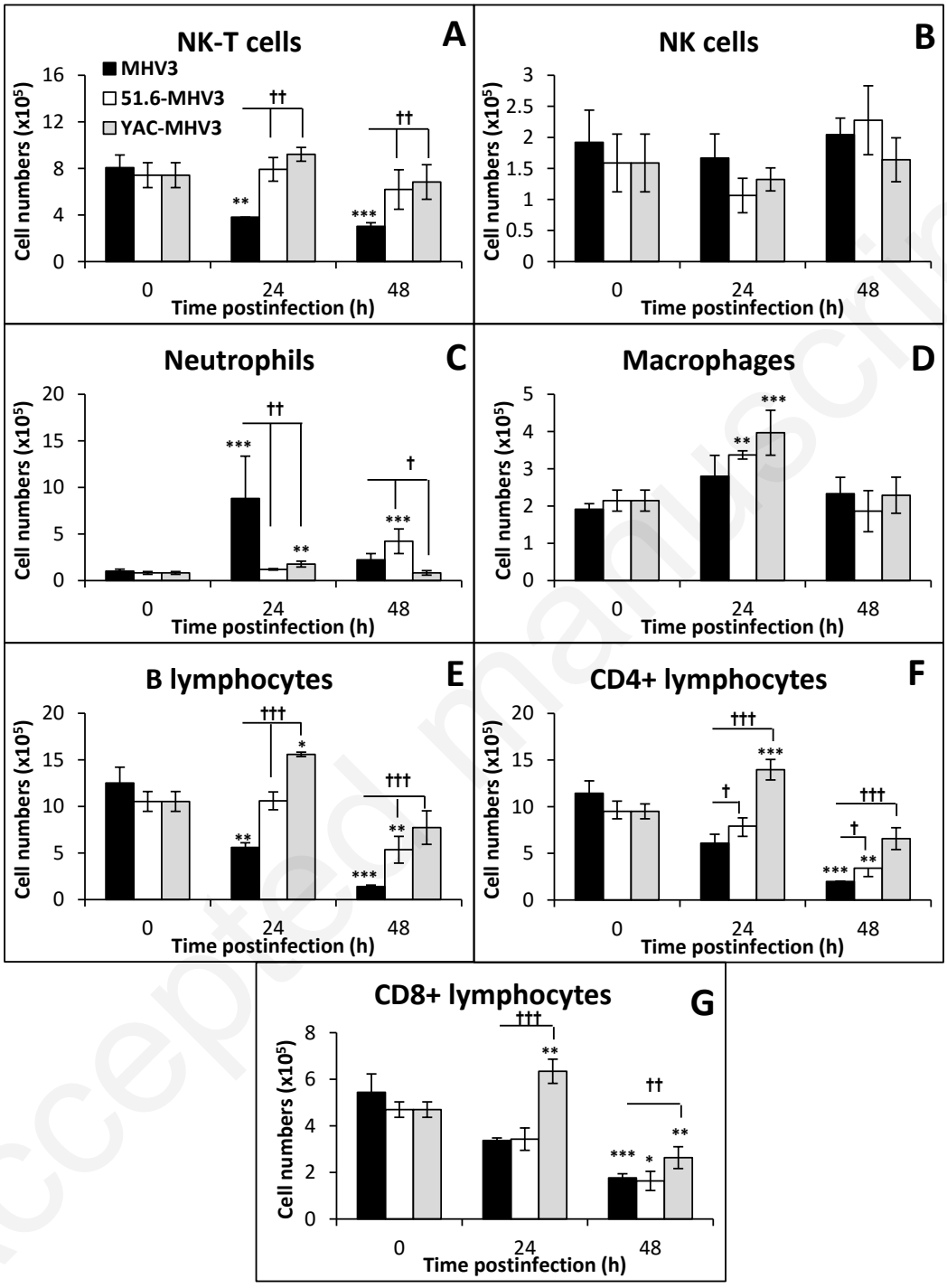

Figure 5
(Section II)

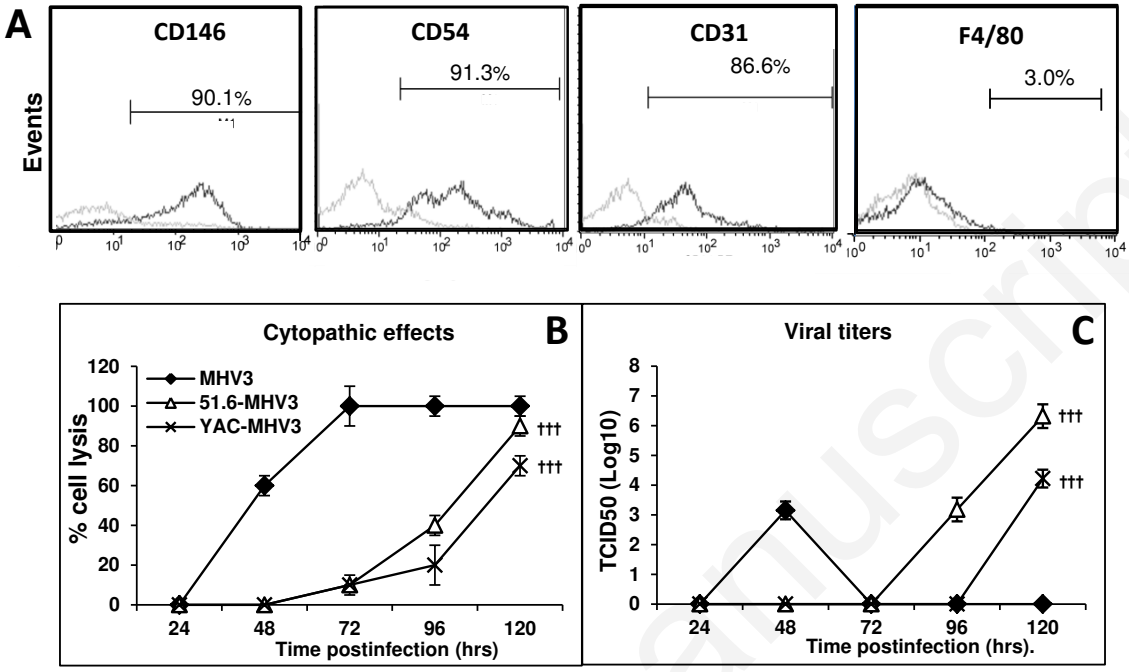

Figure 6

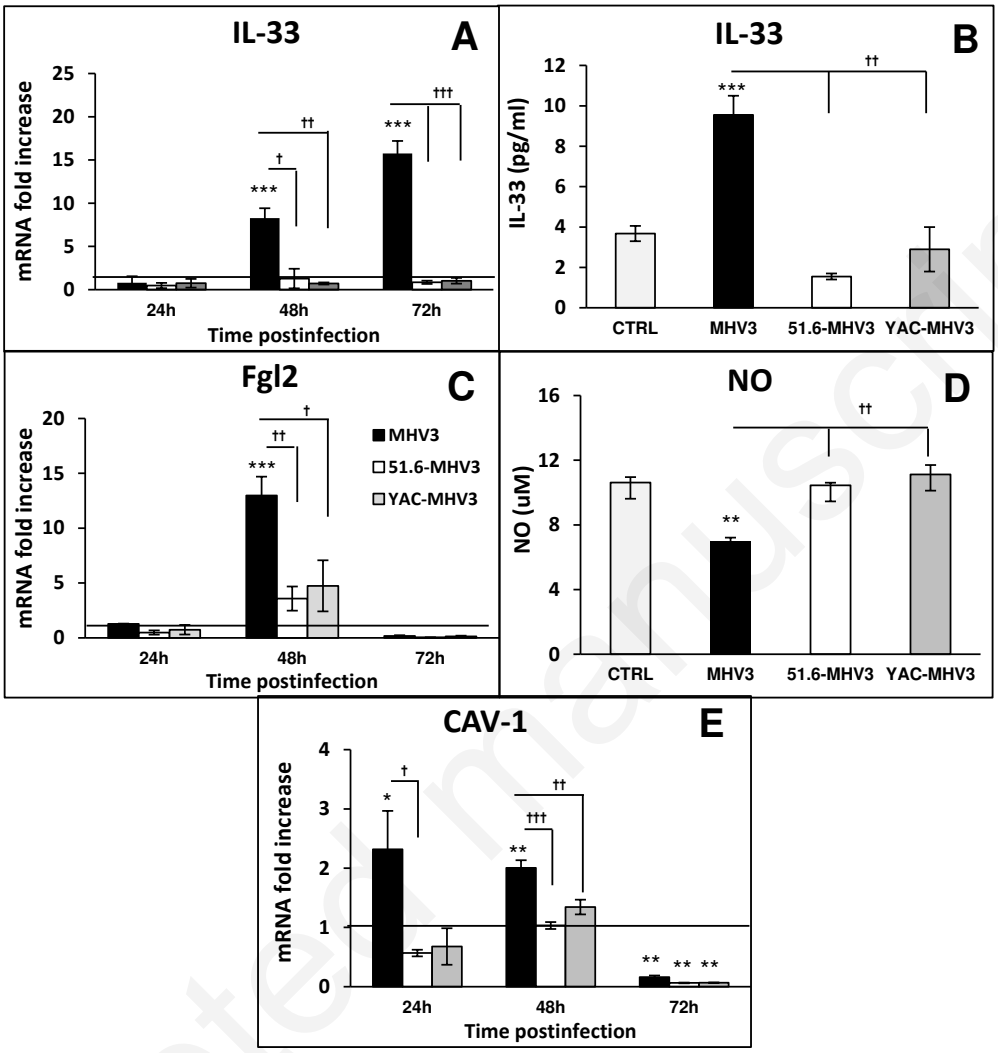

Figure 7

I-

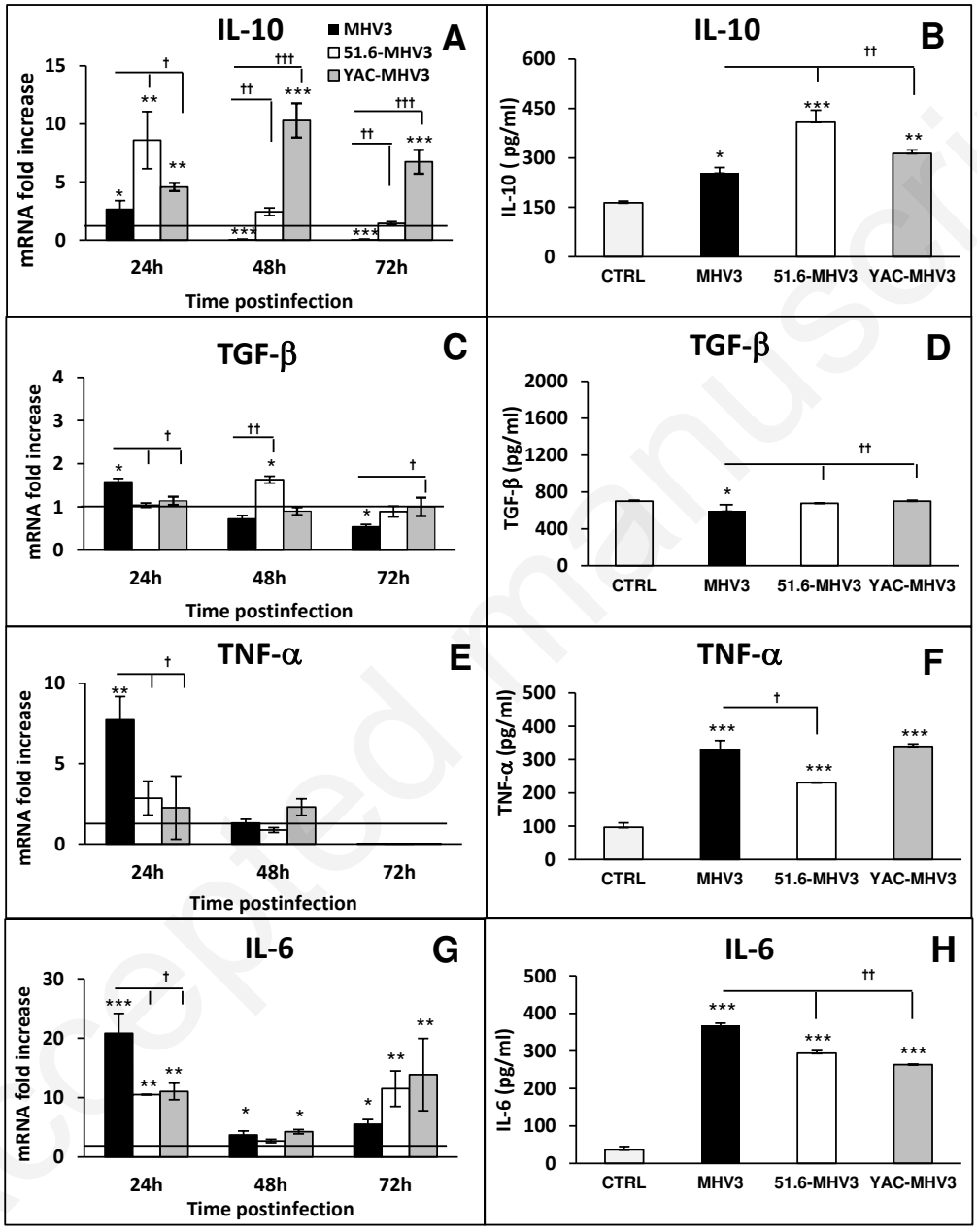

Figure 8
(section I)

II-

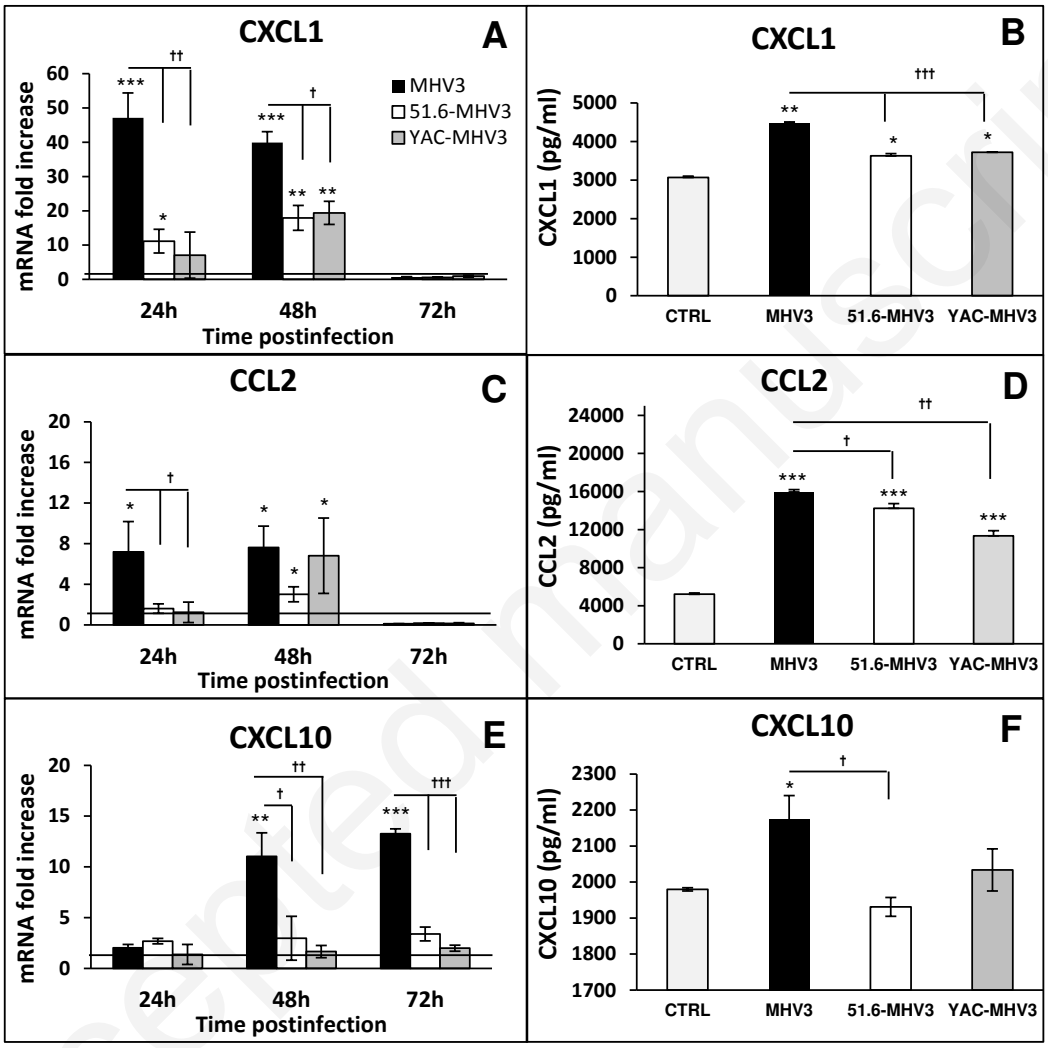

Figure 8
(section II)

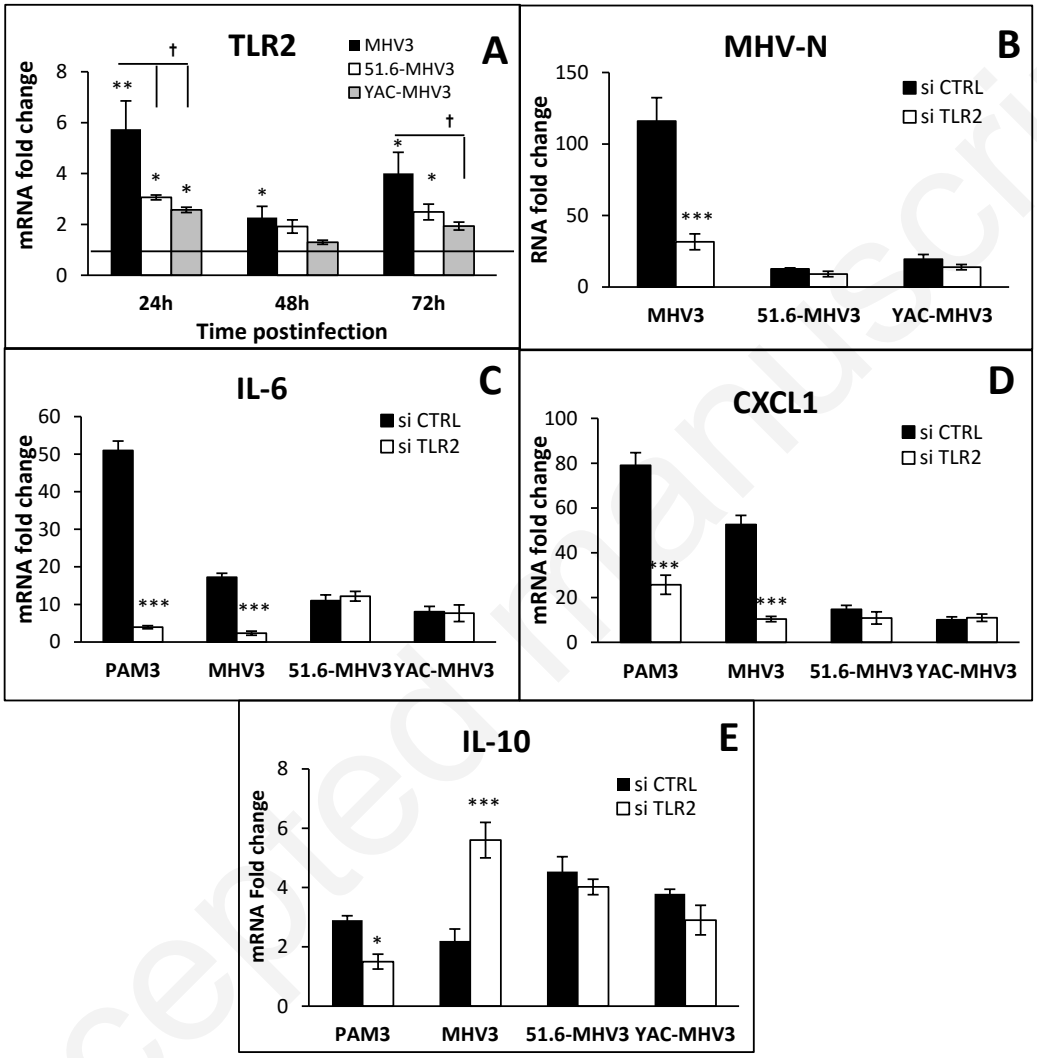

Figure 9

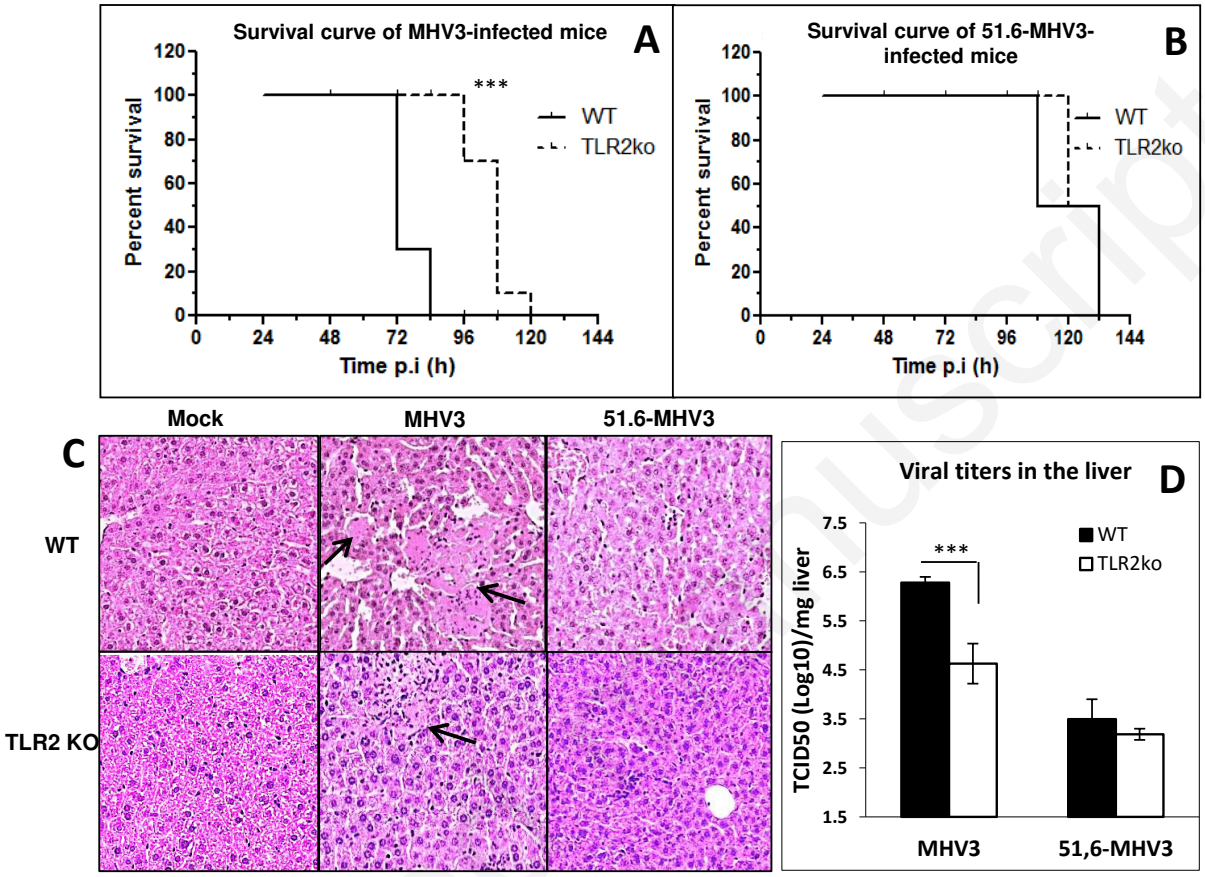

Figure 10

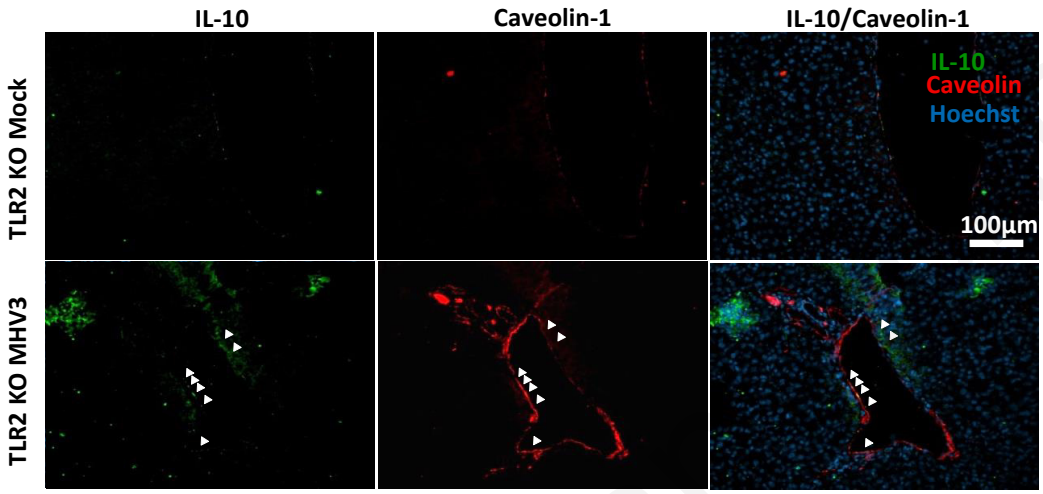

Figure 11

TABLE I : Primers used for quantitative reverse transcription-PCR

Gene	Forward primer	Reverse primer
HPRT	5'-GAAAGACTTGCTCGAGATGTCATG-3'	5'-CACACAGAGGGCCACAATGT-3'
IL-6	5'-TCGGAGGCTTAATTACACATGTTC-3'	5'-TGCCATTGCACAACTCTTTTCT-3'
TNF-α	5'-TCCCAGGTTCTCTTCAAGGGA-3'	5'-GGTGAGGAGCACGTAGTCGG-3'
CCL2	5'-GCAGCAGGTGTCCCAAAGAA-3'	5'-GGTCAGCACAGACCTCTCTCTTG-3'
CXCL10	5'-GGCCATAGGGAAGCTTGAAAT-3'	5'-TCGTGGCAATGATCTCAACAC-3'
ICAM-1	5'-GTCCGCTGTGCTTTGAGAACT-3'	5'-CGGAAACGAATACACGGTGAT-3'
TLR3	5'-TGGGCTGAAGTGGACAAATCT-3'	5'-TGCCGACATCATGGAGGTT-3'
CAV-1	5'-GCGCACACCAAGGAGATTG-3'	5'-CACGTCGTCGTTGAGATGCT-3'
TLR7	5'-CAGTGAACTCTGGCCGTTGA-3'	5'-CAAGCCGGTTGTTGGAGAA-3'
MHV-N	5'-TGGAAGGTCTGCACCTGCTA-3'	5'-TTTGGCCCACGGGATTG-3'
RIG-I	5'-GCCAGAGTGTCAGAATCTCAGTCAG-3'	5'-GAGAACACAGTTGCCTGCTGCTCA-3'
MDA-5	5'-GCCCTCTCCTTCCTCTGAGACT-3'	5'-GCTGGAGGAGGGTCAGCAA-3'
IL-33	5'-GCTGCGTCTGTTGACACATTG-3'	5'-GGGAGGCAGGAGACTGTGTTAA-3'
Fgl2	5'-CGTTGTGGTCAACAGTTTGGA-3'	5'-GATGTTGAACCGGCTGTGACT-3'
CXCL1	5'-CCGAAGTCATAGCCACACTCAA-3'	5'-CAAGGGAGCTTCAGGGTCAA-3'
IL-10	5'-GATGCCCCAGGCAGAGAA-3'	5'-CACCCAGGGAATTCAAATGC-3'
TGF-β	5'-AGCGCTCACTGCTCTTGTGA-3'	5'-GCTGATCCCGTTGATTTCCA-3'

Table II. Transcription levels of several genes in liver from MHV3- and 51.6-MHV3-infected C57BL/6 (WT) and TLR2 KO mice at 72 h p.i.

	MHV3		**51.6-MHV3**	
Genes	WT	TLR2 KO	WT	TLR2 KO
TNF-α	70.2 ± 7.2	44.9 ± 4.0 ***	10.5± 1.03	7.1 ± 2.8
IL-6	43.5 ± 5.7	11.2 ± 5.0 ***	13 ± 1.4	14 ± 7.4
IL-10	5.8 ± 1.4	44 ± 11.7 ***	54.5 ± 17.4	41.4 ± 3.8
CXCL1	131 ± 15	21.1 ± 8.7 ***	107 ± 4.9	91 ± 11.9
CCL2	1027 ± 134	155 ± 37 ***	147 ± 14.8	120.4 ± 39.1
CXCL10	213 ± 20	69 ± 15 ***	33.7 ± 7.4	17.5 ± 4.8 *
Fgl2	6.65 ± 0.70	10.1 ± 1.2	6.7 ± 0.7	4.7 ± 1.7
IL-33	4.5 ± 0.4	3.7 ± 0.3	n.d.	n.d.

Groups of 5 or 6 C57BL/6 (WT) or TLR2 KO mice were intraperitoneally infected with 1000 TCID50 (tissue culture infective dose 50%) of MHV3 or 51.6-MHV3. At 72 h p.i., livers were collected from mock- and viral-infected mice from each group and mRNA fold changes for several genes were analyzed by qRT-PCR. Values represent fold change in gene expression relative to mock-infected mice after normalisation with HPRT expression. Samples from each mouse were run in duplicate. Values that are significantly different between MHV3-infected TLR2 KO and C57BL/6 (WT) mice or between 51.6-MHV3-infected TLR2 KO and C57BL/6 (WT) are indicated by asterisks as follows: ***$P < 0{\cdot}001$ *$P < 0{\cdot}05$. n.d. not detectable.